OULUN YLIOPISTO
UNIVERSITY of OULU

DEGREE PROGRAMME IN WIRELESS COMMUNICATIONS ENGINEERING

OPTIMISATION OF IEEE 802.15.4 FOR SUBURBAN SMART GRID COMMUNICATION IN HYBRID LTE-WSN NETWORK

Author _____
Kamaldeep Singh

Supervisor _____
Dr. Jussi Haapola

Instructor _____
Docent Nandana Rajatheva

Accepted _____ /_____ 2014

Grade _____

Singh K. (2014) Optimisation of IEEE 802.15.4 for suburban smart grid communication in hybrid LTE-WSN network. University of Oulu, Department of Communications Engineering, Master's Degree program in Wireless Communications Engineering. Master's thesis, 57 p.

ABSTRACT

Smart grids (SGs) are empowered with information and communication technologies and have paved the way to the modernisation of the old electric grids. In recent years, SGs have provided many opportunities for smart meter (SM) communications that offer diverse energy management applications. The National Institute of Standards and Technology (NIST) has suggested a framework for smart metering applications which is based on wireless networks. Low-cost wireless sensor networks (WSNs) and the 3rd Generation Partnership Project (3GPP) Long Term Evolution (LTE) (i.e., hybrid LTE-WSN) are considered to be promising solutions to interconnect several intelligent devices in an SG network. The purpose of this thesis was to investigate the feasibility of the pure LTE network and hybrid LTE-WSN approaches for smart metering in a realistic suburban scenario. The medium access control (MAC) layer of the IEEE 802.15.4 standard for smart metering applications was optimised. A mathematical Markov chain model was introduced for an unslotted carrier sense multiple access-collision avoidance (CSMA-CA) mechanism which examines the network throughput and packet delay of the SMs. The network performance of the proposed model was compared to predefined requirements of the NIST for SM communications using Matlab and the Opnet modeler simulator. The results showed that the packet delay and network throughput of SM traffic meet the NIST requirements. The results confirmed the feasibility of the hybrid LTE-WSN approach as a promising solution for SM communications.

Keywords: Smart grids, smart meters, hybrid networks, IEEE 802.15.4, network throughput, packet delay, WSN, LTE, Markov model, Opnet modeler.

TABLE OF CONTENTS

FOREWORD

This thesis is formulated in accordance with our project "Smart Grid and Energy Market" (SGEM) under the task "Traffic requirements and dimensioning for smart grids communications". I would like to thank our project partners from Nokia Siemens Networks (NSN) for their valuable input to make the simulations more realistic in terms of functional and non-functional requirements.

I want to express my sincere gratitude towards my supervisor and instructor Dr. Jussi Haapola for his unconditional guidance, patience, and support. I could never gone this far without his directions. I would also like to express my appreciation and admiration to my second supervisor Docent Nandana Rajatheva and Prof. Matti Latva-aho for their continuous support in my master studies and research. I would like to thanks my friends and lab mates, Aravind Avvaru, Dr. Animesh Yadav, Ganesh Venkatraman, Jasmine Maggo, Janita Klemola, Nuwan S. Ferdinand, Dr. Pradeep Kumar, Sumudu P. Samarakon, Uditha Wijewardhana and Xiaojia Lu. The conversations with these people have always been a great pleasure, and have sparkled a lot of good ideas which eventually became a part of this thesis. I would also like to thank our project mate Juha Markkula for providing the LTE Opnet simulation results.

I would like to dedicate this thesis to my parents for their immense love, sacrifice and encouragement. Lastly and most importantly, I want to thanks almighty Lord for his blessings.

Oulu, January 5, 2014

Kamaldeep Singh

LIST OF ABBREVIATIONS

A-GW	Access gateway
AMI	Automated metering infrastructure
AMR	Automated meter reading
BI	Beacon interval
BE	Backoff exponent
BG	Background
BO	Beacon order
BS	Base station
BER	Bit error rate
CP	Cyclic prefix
CW	Contention window
CAP	Contention access period
CCA	Clear channel assessment
CFP	Contention free period
CLH	Cluster head
CSP	Communication service provider
CQI	Channel quality indicator
CDMA	Code division multiple access
CSMA-CA	Carrier sense multiple access with collision avoidance
DL	Downlink
DFT	Discrete Fourier transform
ED	Energy detection
eNB	Evolved node-B
EPC	Evolved packet core
EPS	Evolved packet system
E-UTRAN	Enhanced UMTS terrestrial radio access network
FCS	Frame check sequence
FDD	Frequency division duplex
FFD	Full functional device
FTP	File Transfer Protocol
FDMA	Frequency division multiple access
2G	Second generation
3G	Third generation
4G	Fourth generation
GBR	Guaranteed bit rate
GSM	Global System for Mobile Communications
GTB	GPRS tunneling protocol
GTS	Guaranteed time slot
GUI	Graphical user interface
3GPP	3rd Generation Partnership Project
GGSN	Gateway GPRS support node
GPRS	General packet radio service
HSS	Home subscriber server
IP	Internet Protocol
ICT	Information and communication technologies

IMS	IP-based multimedia service
IEEE	Institute of Electrical and Electronics Engineers
KP	Kernel procedures
Kbps	Kilobits per second
LLC	Logical link control
LQI	Link quality indicator
LTE	Long-term evolution
LIFS	Long inter-frame spacing
MS	Mobile station
MAC	Media access control
MCR	Modulation and coding scheme
MDM	Meter data management
MFR	MAC footer
MHR	MAC header
MME	Mobility management entity
MCPS	MAC common part sublayer
MIMO	Multiple input, multiple output
MLME	MAC layer management entity
MPDU	MAC protocol data unit
Mbps	Megabits per second
NB	Number of backoffs
NAS	Non-access stratum
NIST	National Institute of Standards and Technology
OFDM	Orthogonal frequency division multiplexing
OFDMA	Orthogonal frequency division multiple access
PD	PHY data service
PAN	Personal area network
PDN	Packet data network
PDR	Packet delivery ratio
PHR	PHY header
PHY	Physical
PIB	PAN information base
P-GW	PDN gateway
PRB	Physical resource block
PAPR	Peak-to-average power ratio
PCRF	Policy control and charging rules
PDCP	Packet Data Convergence Protocol
PLME	PHY layer management entity
PMIP	Proxy mobile IPv6
PPDU	PHY protocol data unit
QAM	Quadrature amplitude modulation
QoS	Quality of service
QPSK	Quadrature phase shift keying
RF	Radio frequency
RFD	Reduced functional device
RLC	Radio link control
RRC	Radio resource control

RRM	Radio resource management
RTU	Remote terminal unit
RTT	Round trip time
SD	Superframe duration
SG	Smart grid
SM	Smart meter
SO	Superframe order
SAE	System architecture evolution
SAP	Service access point
SHR	Synchronization header
SIP	Session Initiation Protocol
S-GW	Serving gateway
SNR	Signal-to-noise ratio
STD	State transition diagram
SDMA	Spatial-division medium access
SIFS	Short inter-frame spacing
SINR	Signal-to-interference-and-noise ratio
SSCS	Service specific convergence sublayer
SC-FDMA	Single carrier frequency division multiple access
TDD	Time division duplex
TDM	Time division multiplexing
TPC	Transmit power control
TTI	Transmission time interval
TDMA	Time division multiple access
UE	User equipment
UL	Uplink
UMTS	Universal Mobile Telecommunications System
UTRA	Universal terrestrial radio access
UTRAN	Universal terrestrial radio access network
WSN	Wireless sensor network
WLAN	Wireless local are network
WPAN	Wireless personal area network
ZB	ZigBee

LIST OF SYMBOLS

BE_{max}	Maximum backoff exponential
BE_{min}	Minimum backoff exponential
$b_{i,k}$	Markov chain steady state probabilities
$c(t)$	Backoff time counter for a given station at time t
d_{pl}	Distance in free space pathloss model
D	Average delay for node
$E(slot)$	Duration of backoff slot (aUnitBackoffPeriod)
$E[X]$	Average backoff delay
$E[W_i]$	Average successfully transmitted time slot at $i-th$ stage
f_c	carrier frequency in MHz
h_{BS}	BS antenna height in *m*
h_{MS}	MS antenna height in *m*
i	Denotes stochastic process $c(t)$
k	Denotes stochastic process $s(t)$
m	Maximum CSMA backoff number
n	Number of devices or nodes
S_{pl}	Macrocell suburban model
t_b	Average number of busy slots
t_o	Average number of backoff slots
T_{ACK}	Number of slots for receiving an acknowledgement
T_c	Number of occupied slots for collision
T_{CCA}	Number of slots for performing CCA
T_L	Number of slots for transmitting a packet
T_s	Number of slots for successful transmission
T_{bs}	Number of busy slots counted for T_{os}
T_{bc}	Number of busy slots counted for T_{oc}
T_{os}	Average backoff slots in successful transmission
T_{oc}	Average backoff slots during collison
δ	Number of slots waiting for an acknowledgement
ϕ	Probability of sensing the channel
λ	Wavelength in free space pathloss model
γ	Probability that device transmits successfully after a CCA
pl	Total length of the packet
p	Probability of busy channel
P_{so}	Probability that the transmission is successful
P_{to}	Probability that the given device does not perform a CCA
ϕ	Probability of sensing the channel
S	Throughput
s_i	Backoff time stage for a given station at time t
$s(t)$	Probability that a node successfully sends a frame at $i-th$ stage
W	Minimum contention window size
W_0	Contention window size at $0-th$ backoff stage
W_1	Contention window size at $1st$ backoff stage
W_m	Contention window size at $m-th$ backoff stage
W_i	Contention window size at backoff stage i, i.e. $W_i = 2^i W$, $i\epsilon(0, m)$

1. INTRODUCTION

Recent years have seen smart grids (SGs) revolutionise electrical metering systems, which are now integrated with fast communication and intelligent technologies. SGs are being visualised to enhance power grids in terms of supply reliability and cost-effective control of transmission, distribution, and electricity consumption [1–3]. SGs can visualise electricity information (e.g. smart automated meter data, monthly electricity charges, and electricity usage recommendation) for both utility companies and consumers. An SG is a high-speed and bidirectional electricity network equipped with advanced information, control, and communication technologies [1,2]. Automated metering is an SG subsystem which plays a major role in SG infrastructure and wireless applications [3]. SGs provide comprehensive opportunities for automated meter reading (AMR) to calculate the energy expenditure using automated metering infrastructure (AMI). The AMI system combines three elements: smart meters (SMs), metering communication infrastructure, and a meter data management (MDM) system [4]. The SM is an electrical device and is mostly deployed on the consumer's premises to collect data on the energy usage, power outage, and quality notification [5]. The MDM system stores and manages vast quantities of data which are delivered by various smart metering systems. The basic function of MDM system is to import and process the data before making it available for billing and other analytic research [6, 7].

The metering infrastructure supports the communication requirements of SGs [7]. The National Institute of Standards and Technology (NIST) has suggested some of the key communication networks for enabling smart metering applications, such as Long Term Evolution (LTE) and wireless sensor networks (WSNs) [8]. LTE is considered to be a potential candidate for handling SM communication and provides ubiquitous wide area coverage, high availability, and strong security [3]. An LTE network will provide quick and reliable load and outage information, which will help utility companies manage their resources [9]. However, implementing LTE in SMs poses challenges such as address depletion, traffic scheduling and reduced mobility management [10]. A WSN comprises multi-functional, cost-efficient, and low-power sensors and can be used as a communication solution for monitoring and controlling applications in SMs. In this thesis, the possibility of using a hybrid LTE-WSN approach for real-time smart metering applications was evaluated.

Figure 1 depicts a typical system model for SM communication using a hybrid LTE-WSN approach in a suburban region. The multi-functional sensors integrated with SMs are strategically deployed into suburban clusters. The cluster head (CLH) coordinates the clusters. The main function of the CLH is to accumulate and aggregate the electricity usage information from the SMs. The CLH is equipped with an LTE-capable relay and transmits the information to LTE base stations (eNBs) using the long-range transmission. SM data are stored in a remote server and forwarded to the utility companies for billing.

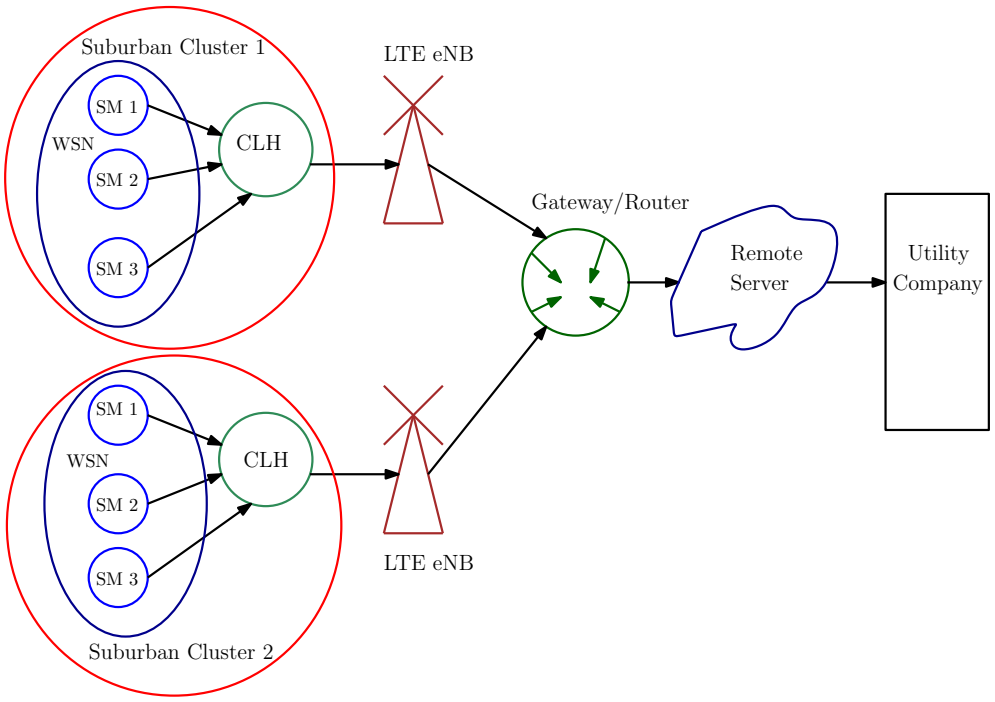

Figure 1. Typical hybrid LTE-WSN suburban environment.

The critical requirements for smart metering communication are reliability and low latency. The ZigBee/IEEE 802.15.4 standard of WSN has been proven to provide scalability and low packet latency in SG communications [11]. The IEEE 802.15.4 specification suggests default MAC layer parameters such as the minimum backoff exponent, maximum backoff exponent, and maximum CSMA backoffs. However, these parameters may not provide the appropriate tradeoff between the network load and packet latency for all applications [12, 13]. In addition, the analysis is bounded to an unslotted IEEE 802.15.4 as it experiences low network overhead [14], which is the main requirement for smart metering application.

1.1. Motivation

Recent research has focused on AMR devices for smart metering applications using 3G/4G networks [15]. Since LTE provides low latency and high data rates, it is considered to be a promising solution for SGs [16]. However, pure LTE brings a plethora of other issues, including address depletion, congestion control, and reduced mobility management of SGs [10]. In addition, the harsh and complex environment of SG communication poses challenges to the quality-of-service (i.e. low latency) of WSNs [17]. Smart metering requires low latency and high data rates [8]. The hybrid LTE-WSN approach has the potential to provide a platform with reliable communication, low latency, and a high data rate for smart metering applications.

1.2. Scope of Thesis

The main objective of this thesis was to examine feasibility of the pure LTE network and hybrid LTE-WSN approaches for smart metering applications. The proposed model (i.e., hybrid LTE-WSN) was evaluated according to the NIST requirements for smart metering applications. The impact of SM traffic on LTE and WSN was visualised. The work included (i) designing an unslotted IEEE 802.15.4 Markov chain model for suburban smart metering applications; (ii) implementing the model in a Matlab simulator; and (iii) modifying the Opnet open-ZigBee simulator model to verify the network performance of the SM communication.

1.3. Structure of Thesis

The thesis is organized as follows. Chapter 1 briefly discusses SGs and SMs and introduces the hybrid LTE-WSN approach for communication among various SMs and the base station. Chapter 2 describes various traffic scenarios and the simulation setup for suburban smart metering applications. A detailed overview is given of the propagation model and traffic scenarios used in the simulations. Chapter 3 discusses the Opnet modeler simulator and depicts various network topologies and the simulation environment. Chapter 4 addresses the IEEE 802.15.4 standard and its architecture. The network throughput and packet delay of unslotted IEEE 802.15.4 was evaluated using the Markov chain analysis tool. Chapter 5 describes the LTE network architecture, LTE propagation model, simulation parameters, and LTE traffic simulation results. Chapter 6 concludes the thesis.

2. SCENARIO DESCRIPTION

2.1. Introduction

The chapter describes various traffic scenarios in a suburban region. A detailed overview is given of the propagation models and terrain attributes which were used in the simulations. The suburban region largely consisted of houses instead of apartment blocks (buildings); thus, it had a lower density of remote terminal units (RTUs) [15].

The suburban area was divided into 30 clusters (group of buildings); each contained 25 (750 total) houses with AMR units. Two approaches were examined for their suitability to SG metering: pure LTE network and hybrid LTE-WSN. In pure LTE, each house has one RTU which is connected with an LTE-network evolved node-B (eNB) [15, 18]. The RTUs are randomly placed inside every cluster at the start of each simulation [15,18]. The AMR units are placed randomly at various locations. In hybrid LTE-WSN, SMs form communication clusters with a single LTE-capable relay. The cluster head (CLH) contains both IEEE 802.15.4 and LTE communication interfaces. The advantage of this topology is that it decreases several RTUs in the LTE network and maintains large-area connectivity with an additional hop [15]. Figure 2 shows the simulation topology with the LTE-WSN approach.

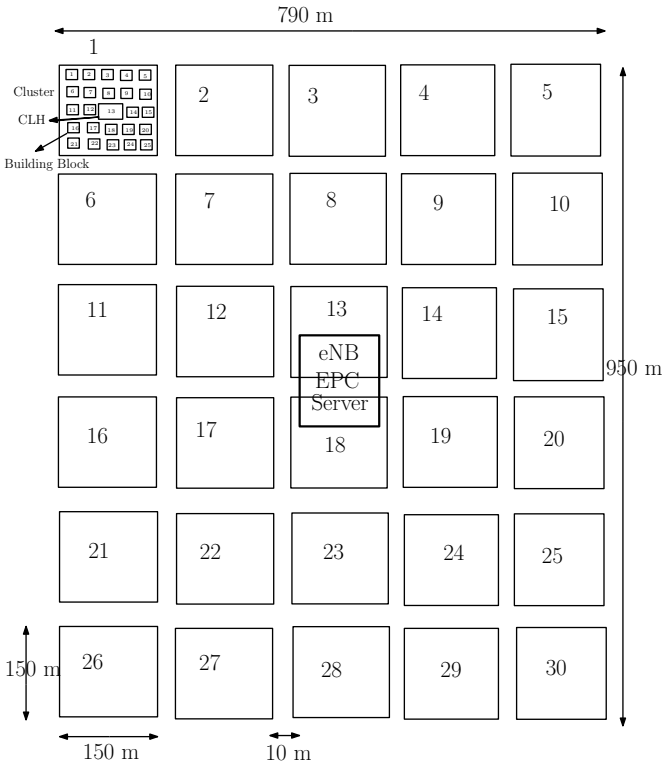

Figure 2. Evaluated topology with 30 CLHs (LTE-WSN approach).

2.2. Propagation Models

Indoor losses were not modelled for the LTE and IEEE 802.15.4 propagation channels, because the signal propagates only a few metres [15]. However, outdoor losses (e.g. building entry losses) are considered to be a critical source of attenuation [15].

The focus of this thesis was on finding a suitable radio propagation model of the LTE and WSN communication networks for a suburban scenario. The primary goal was to focus on the generic channel modelling aspects of SGs. When deployed in a suburban environment, the channel model for SG devices comprises the outdoor and indoor propagation of radio signals [18]. Radio waves transmitted by an eNB to SG devices propagate to the building external wall and inside the building to the device [18, 19]. Losses from outdoors to indoors were estimated using the pathloss model of the Opnet simulator. Only losses which were caused by walls were estimated since they are the primary source of attenuation [20]. Each wall attenuated the signal by approximately 6 dB to cause slow fading [15, 21].

2.2.1. WPAN Propagation Model

A predefined Opnet simulator free space pathloss model was selected for IEEE 802.15.4. The free space pathloss model is defined as follows [22]:

$$d_{pl} = (\frac{\lambda}{4\pi d})^2 \tag{2.1}$$

where d_{pl} is the distance and λ is the wavelength; both are in *metres*.

2.2.2. LTE Propagation Model

The orthogonal channels in LTE encounter narrowband fading. In order to evaluate the channel propagation effects, a narrowband channel model was determined for the suburban smart metering scenario. One such pathloss model is the suburban macrocell model developed by 3GPP, which uses a modified COST231 HATA model [18, 22]. The Opnet modeler version 16.0 with its LTE specialized model [18] was chosen to be the simulator. The suburban macrocell pathloss model was selected as it was the best suited for the stated network topology. The pathloss expression S_{pl} for the macrocell suburban model is defined by the following equation [15, 20]:

$$\begin{aligned} S_{pl}[dB] \quad &= (44{,}9 - 6{,}55log(h_{BS}))log(d/1000) \\ &+45{,}5 + (35{,}46 - 1{,}1h_{MS})log(f_c) \\ &-13{,}82log(h_{BS}) + 0{,}7h_{MS} + C \end{aligned} \tag{2.2}$$

where h_{BS} is the base station (BS) antenna height in *metres*, h_{MS} is the mobile station (MS) antenna height in *metres*, f_c is the carrier frequency in *megahertz*, *d* is the distance between BS and MS in *metres*, and *C* is a constant factor [18, 20]. Terrain

category c was chosen for the simulations [18].

The BS antenna height h_{BS} was 10-85 *metre*. The values of a-c depend on the terrain category. Shadow fading is caused by obstacles between the transmitter and receiver which attenuate power through absorption, scattering, reflection, and diffraction [23]. The standard deviation of the shadow fading was assumed to be zero.

2.3. Terrain Attributes

The terrain type attributes were considered when the pathloss model was fixed as suburban. The suburban fixed pathloss model was set to one of the three most common types of terrain [24]:

- a: hilly terrain with moderate-to-heavy tree densities [24].
- b: compromise between terrains *a* and *c*.
- c: mostly flat terrain with light tree densities.

2.4. Traffic Scenarios

In this thesis, different traffic scenarios were investigated to identify the best network approaches for SM traffic in a suburban region. The traffic scenarios covered in the simulations are presented below.

2.4.1. Normal AMR Traffic

In this simulation scenario, all 25 RTUs transmit AMR traffic to a server located somewhere beyond the evolved packet core (EPC) [18,20]. Table 1 presents the AMR traffic generation parameters [20]. The simulation was run for 1 h with a payload of 250 bytes per RTU.

Table 1. NORMAL AMR TRAFFIC GENERATION PARAMETERS PER RTU

Data Type	Start Time	Generation Interval	Payload Data	Simulation Duration
AMR data	Random 5-20 min	15 min	250 Bytes	1 h

2.4.2. Background Traffic

The typical traffic present in LTE is defined as background (BG) traffic [18,20]. Applications which generate BG traffic in LTE include voice, video, streaming, web, FTP, and data usage, as shown in Table 2 [20].

Table 2. BG TRAFFIC APPLICATIONS

Parameters (per subscriber)	Session length/size
Voice	2.5 min
Video	0.05 min
Streaming	1 min
Web	2 pages
FTP	2914 kB
Data usage	5 MB/h

Table 3 [20] presents the generated BG traffic per cluster and in total. There were 30 clusters containing a total of 930 BG nodes. In order to reduce the simulation time, only one node generated BG traffic per cluster in this scenario. However, the volume of traffic was the same as the total generated by 31 user equipments (UEs).

Table 3. GENERATED BG TRAFFIC OVER 55 MIN

BG traffic	Per cluster (MB)	Total (MB)	Total (MB/s)
Uplink (kB)	16.4	492.8	0.15
Downlink (kB)	125.3-127.8	3759.2-3833.6	1.14-1.16
Total	142.7-144.2	4252-4326.4	1.29-1.31

2.4.3. Two-Way Normal AMR Traffic with BG Traffic

In this scenario, the server also generates AMR data (tariff updates, reconfiguration, etc.) in the downlink direction [18,20]. Table 4 presents the traffic generation parameters for the simulation scenario [20]. The server generates 25 packets evenly between the clusters, i.e., 1 packet is generated for each RTU with a repeating cycle [18,20]. In addition, the downlink packet generation is evenly distributed throughout the generation time interval [18,20].

Table 4. TRAFFIC GENERATION PARAMETERS

Data Type	Start Time	Generation Interval	Payload Data	Simulation Duration
AMR data (uplink)	Random 5-20 min	15 min	250 Bytes	1 h
AMR data (downlink)	5 min	4.3 s	250 Bytes (750 packets)	

3. OPNET SIMULATOR

3.1. Opnet Modeler: Background and Overview

Network simulation is a way to model various communication networks and test their performances. The Opnet modeler is a network-level event-based simulation tool which can modify various network attributes to check the behaviour of the network under different conditions. The Opnet simulator consists of an extensive set of libraries of accurate and reliable communication models which are commercially available as fixed network hardware and protocols [24]. In addition, the Opnet simulator offers model design, simulation, data mining and analysis. It can simulate a wide variety of networks and link to each other [24].

The Opnet modeler has advanced simulation capabilities and an extensive protocol model which are suited for designing and optimising wireless protocols [24]. Furthermore, the wireless model not only supports cellular networks like the Global System for Mobile Communications (GSM), Universal Mobile Telecommunications System (UMTS), LTE, mobile ad-hoc network, wireless local area network (WLAN), and personal area networks (Bluetooth, ZigBee (ZB), wireless personal area network (WPAN), etc.) but also incorporates motion in mobile networks. Moreover, the wireless model enables analysis of end-to-end behavior, network performance, and different network scenarios.

Opnet provides a hierarchical structure for network modelling [25]. This allows low-level models to be reused. A hierarchical model comprising three levels is presented below.

Network Model

The network model is the top-level model and is used to specify a network topology. It defines the physical (PHY) position of the communication entities (i.e. nodes) and their interconnections (i.e. links). In addition, each node can be fixed, mobile, or satellite; and their parameters can be changed independently from other nodes which are participating in the network [26]. Radio links do not exist as objects in a network model. These radio links are dynamically established between some or all nodes in a network depending on PHY layer parameters such as the frequency band, modulation scheme, transmitter power, and distance. The parallel radio link to each receiver is called a radio transceiver pipeline [25].

Node Model

The communication entities which are participating in the network model need to be specified in the node domain. Each node model consists of a number of interconnected modules, as shown in Figure 3 [24]. These modules are referred to as processors and queues [24]. The interconnections between modules can be packet streams, statistic wires, or logical associations. The packet streams transfer the packets or formatted messages between modules, and the statistic wires carry control information between the modules [27].

Process Model

The process model describes the behaviour of the user-defined modules. This behavior can simulate a wide variety of communication subsystems, such as communication protocols, traffic generators, and statistic collectors. The behaviour of the process is defined by the process editor, which is specially designed for developing protocols and algorithms. These processes are defined by a combination of the state transition diagram (STD), set of kernel procedures (KP), and general C/C++ code [24]. The process model can be defined graphically by STD, which consists of the number of states and transitions, as presented in Figure 4 [24].

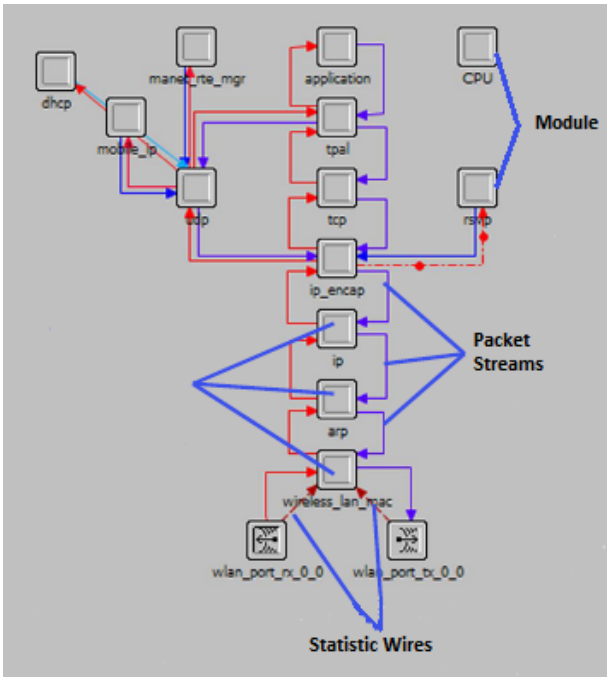

Figure 3. Structure of node model.

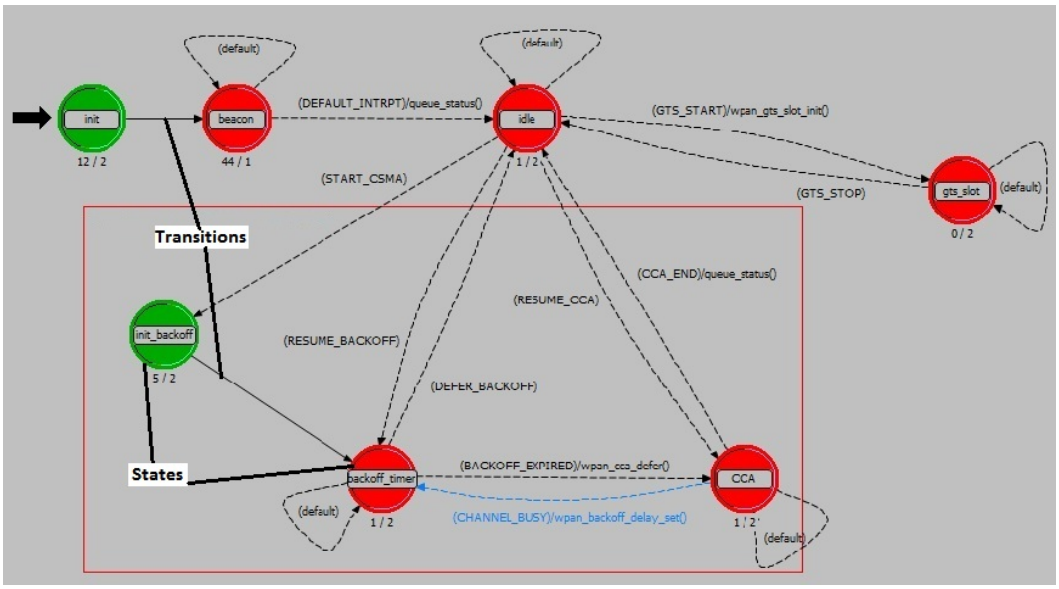

Figure 4. Structure of process model.

3.2. Simulation Environment and Setup

The simulation scenario describes a suburban environment with many houses, some row houses, and a few low-rise apartment block buildings [15]. The terrain is quite flat in the region, and buildings are clustered [15]. The cluster dimensions are roughly 150 m $\times$ 150 m, and each contains approximately 25 buildings. The area contains about 30 such clusters in a space of 2.5 km $\times$ 1.5 km [15, 18]. The area should have about 750 AMR RTUs in total. A network topology with 25 RTUs and one CLH was used in the simulations.

Figure 5 presents the Opnet simulation environment where 25 RTUs send traffic (data packets) to the CLH in a cluster. In the stated network topology, the CLH does not broadcast the data packets but receives the data from each RTU. Furthermore, the mobility model randomly places each RTU in a cluster. However, the position of the CLH is fixed and is situated in the middle of the topology. The configuration parameters of CLH and RTU are shown in Figures 6 and Figure 7, respectively. Figure 6 depicts the chosen parameters for the CSMA-CA MAC layer, whereas Figure 7 presents the selected parameters for application to traffic.

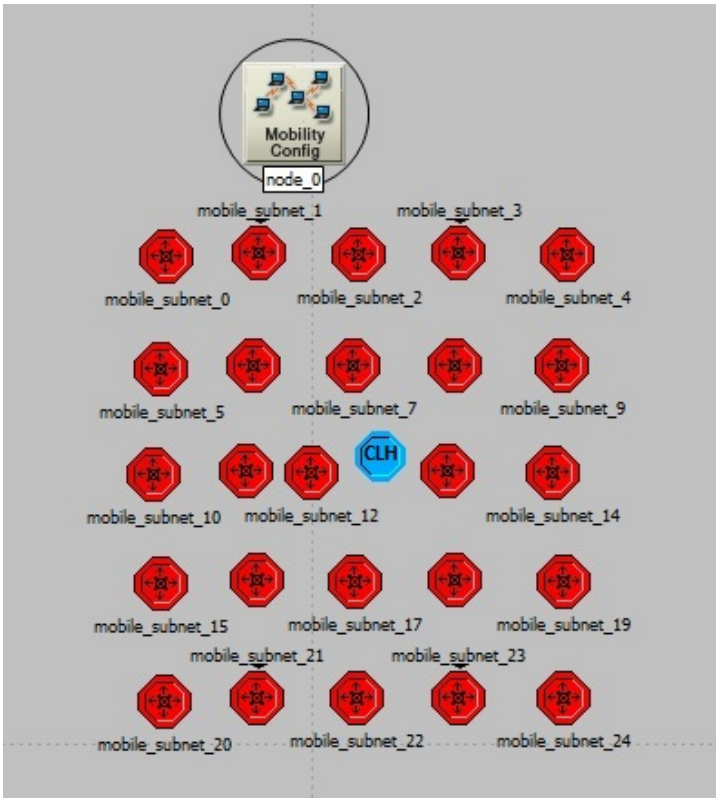

Figure 5. Network topology.

Attribute	Value
name	PAN coordinator
ZigBee Parameters	
MAC Parameters	
Beacon Order	15
Best Effort Buffer Capacity	1000
CSMA Parameters	(...)
Maximum Backoff Number	9
Minimum Backoff Exponent	5
Battery Life Extension	disabled
Number of Retransmissions	5
PAN ID	0
Superframe Order	15
Network Parameters	
Device Mode	PAN coordinator
MAC Address	0
PHY Parameters	
Application Traffic	
Best Effort (CAP)	disabled
Destination Address	broadcast
Real-Time (CFP)	disabled
Battery	

Figure 6. CLH simulation parameters.

Attribute	Value
name	RTU_22
Application Traffic	
Best Effort (CAP)	(...)
Start Time (sec)	300
Stop Time (sec)	end of simulation
Packet Interarrival Time (sec)	constant (4.3)
Packet Size (bit)	constant (2000)
Acknowledgment	enabled
Destination Address	0
Real-Time (CFP)	(...)
ZigBee Parameters	
MAC Parameters	
Best Effort Buffer Capacity	1000
CSMA Parameters	(...)
Maximum Backoff Number	9
Minimum Backoff Exponent	5
Battery Life Extension	disabled
Number of Retransmissions	5
Network Parameters	
Device Mode	end device
MAC Address	auto assigned

Figure 7. RTU simulation parameters.

In the simulations, only uplink traffic was considered. The beacon order *(BO)* and superframe order *(SO)* were set to 15 for non-beacon enabled mode. The CSMA parameters (i.e. maximum backoff number, minimum backoff number, and number of retransmissions) were selected after various values were simulated under the condition of maintaining the packet delivery ratio (PDR) close to 99%. The NIST requirements specify that the average delay for smart metering applications should be less than 10 s for payloads of 200-1600 bytes with a PDR of 99% [28]. Table 5 [8] presents the NIST requirements for smart metering applications.

Table 5. NIST REQUIREMENTS FOR SMART METERING APPLICATIONS

NIST requirements for smart metering applications		
Parameters	Values	
Average delay (s)	< 10	
Average payload (bytes)	200 to 1600	
Use cases	MR-14, MR-16, MR-26, MR-27, MR-35.	
Reliability	99 %	
Smart meters using LTE technology		
Parameters	Uplink	Downlink
Average delay (s)	3E-02	3E-03
Average payload (bytes)	250	250
Data load (bits/s)	0.3K	0.08K
Smart meters using WSN technology		
Parameters	Downlink	
Average delay (s)	16	
Average payload (bytes)	250	
Data load (bits/s)	50	

4. DESIGN AND OPTIMISATION OF IEEE 802.15.4

The chapter presents the IEEE 802.15.4 standard architecture and outlines the functionality of different layers such as PHY and MAC. A Markov chain model is proposed for the IEEE 802.15.4 standard in order to establish SM communication. An Opnet open-ZB simulator model was modified to verify the network performance of the SM communication. The performance of the proposed model was evaluated using Matlab and the Opnet modeler simulator.

4.1. Survey on IEEE 802.15.4

The WSN is a collection of nodes with the ability to sense, compute, and communicate. IEEE 802.15.4 is a communication standard for low-data rate, low-power consumption, and low-cost WPANs which require limited battery consumption. Hence, it is intended for industrial, medical, military, agricultural, and residential applications. IEEE 802.15.4 networks share most of the design principles (i.e. PHY and MAC layer architecture) of the WSN; therefore, it can be treated as a member of both WPAN and WSN.

The ZB standard concentrates on the development of the upper network and application layers, whereas IEEE 802.15.4 defines the PHY and MAC layers. The IEEE 802.15.4 standard defines two device types: full function device (FFD) and reduced function device (RFD).

Full Function Device

The FFD supports all mandatory features defined by the IEEE 802.15.4 standard and can take any role in the network. The FFD mainly acts as a personal area network (PAN) coordinator, which provides the beacon transmission in a beacon-enabled network; however, it can also act as a simple device. The coordinator manages the network formation and device authorisation. The FFD can communicate with other FFDs as well as RFDs, but the RFD can only communicate with the FFD.

Reduced Function Device

The RFD has limited memory and processing ability; thus, it takes very basic roles in networks such as measurement and remote control. These devices can be used in sensors and actuators.

4.1.1. IEEE 802.15.4 Network Topologies

The topology established the connections between devices participate in a network. IEEE 802.15.4 mainly supports two types of network topologies: star and peer-to-peer.

Star Topology

Figure 8 shows the star topology: communication is established between the coordinator and the associated devices. Star topology can support a small network coverage area. In addition, the associated devices communicate not among themselves but through the PAN coordinator.

Peer-to-Peer Topology

Figure 8 also shows the peer-to-peer topology: the FFD can communicate with other devices provided that they are in radio range. The advantage of this type of topology is its robustness as it offers high reliability with multiple redundant paths. If any communication link fails, alternate paths can be used without network reorganization. The main disadvantage of this type of topology is its complexity as it requires a network layer, which implements complex routing algorithms.

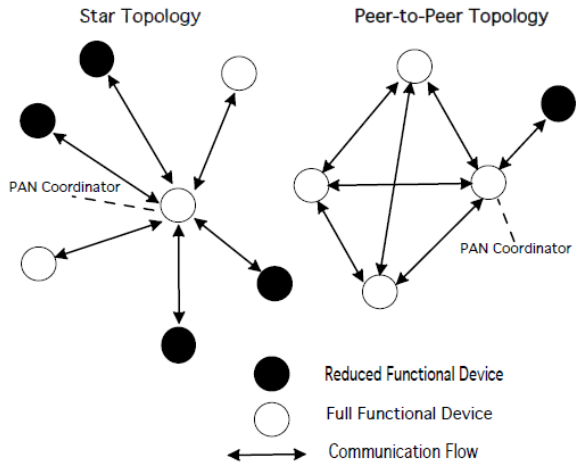

Figure 8. Star and peer-to-peer topologies.

4.1.2. IEEE 802.15.4 Network Architecture

The IEEE 802.15.4 architecture defines the number of blocks; these blocks are called layers. The IEEE 802.15.4 standard also defines the PHY and MAC layers of the low-rate (LR)-WPAN [29]. Figure 9 presents the layer architecture of IEEE 802.15.4 [29].

The PHY layer consists of a radio frequency (RF) transceiver and manages the frequency functionality of LR-WPAN devices; the MAC layer acts as a bridge between PHY and upper sub-layers using the channel access mechanism. In addition, the PHY layer provides services with two service access points (SAPs): PHY layer data service SAP (PD-SAP) and PHY layer management entity SAP (PLME-SAP). PD-SAP is responsible for the transmission and reception of PHY protocol data units (PPDU) across the PHY medium [30]. The MAC layer accesses the upper layers through the MAC common part sub-layer-SAP (MCPS-SAP) or MAC layer management entity-SAP (MLME-SAP) mechanisms. The two SAP mechanisms, service-specific convergence sub-layers (SSCSs) and logical link controls (LLCs), enable the MAC layer to communicate with the upper layers. Figure 9 [29] shows a graphical representation of these layers.

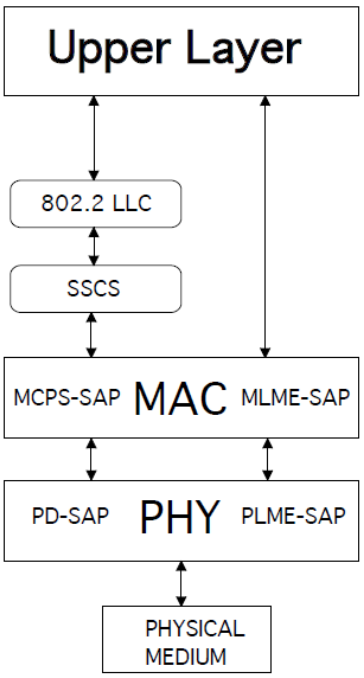

Figure 9. Layered architecture of IEEE 802.15.4.

4.1.3. Physical Layer

The PHY layer provides an interface between the MAC layer and the PHY radio channel. The PHY layer is responsible for data transmission and reception of PPDUs across the PHY radio channel [29, 31].

The LR-WPAN specifies 868/915 MHz and 2.4 GHz frequency bands. Each frequency band has its advantages and disadvantages. The 2.4 GHz frequency band is available worldwide. This band has advantages over the 868/915 MHz frequency band as it has a big market and minimises the production cost of the hardware devices. The main problem with using the 2.4 GHz frequency band is interference due to increasing use of this license band; in contract, the 868/915 MHz frequency band has less propagation losses and larger interference area, which extends the range for a given link budget [32].

PHY Layer Functions

1. Concept of primitives

Figure 10 [29] shows the service hierarchy and two correspondent users with their peer protocol entities. The functions explained below are used to define the concept of primitives.

a) **Request:** A service is initiated.
b) **Indication:** The User is notified about an internal event.
c) **Response:** This completes a procedure that was previously invoked by an indication primitive.
d) **Confirm:** The results of associated service requests are conveyed.

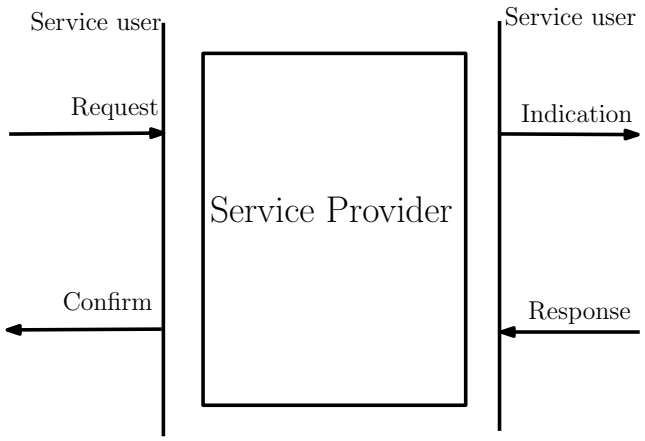

Figure 10. Service hierarchy (primitives).

2. Receiver energy detection (ED)

The receiver ED is used to estimate the receiver signal power within the bandwidth of the channel. The ED duration is equal to 8 symbol periods [29]. The received power value should be at least 40 dB.

3. Clear channel assessment (CCA)

The CCA can be performed by the following methods:

a) Upon detecting the energy above an ED threshold, the CCA reports a busy medium.
b) The CCA reports a busy medium after detecting an IEEE 802.15.4 signal with an energy above the ED threshold.

4. Link quality indication (LQI)

Measuring the LQI gives an indication of the quality of the received packets. The LQI can be measured by using the receiver ED, which is a signal-to-noise estimation method. The LQI results are used in the network or application layer.

5. PPDU format

Figure 11 shows the PPDU frame format [31]; the preamble and start of the frame delimiter are part of the synchronization header (SHR). The preamble field is useful for chip and symbol timing recovery. The preambles are also designed for coarse frequency adjustment in some cases. The start of the frame delimiter is the field which points out the termination of SHR and start of packet data. The PHY header (PHR) gives information about the payload length.

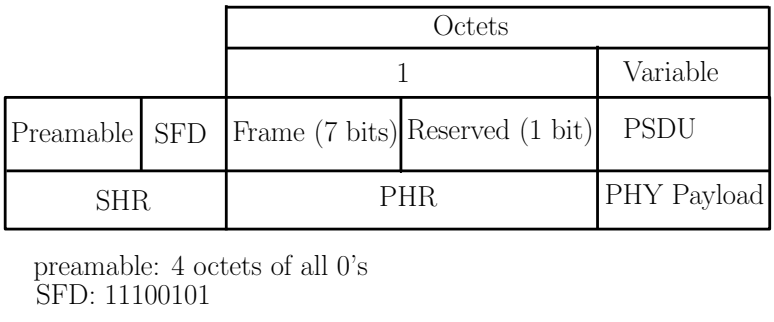

Figure 11. PPDU frame format.

A PPDU packet consists of the SHR, PHR, and payload.
a) **SHR:** allows synchronization of a receiving device.
b) **PHR:** contains the frame length information.
c) **Payload:** carries the MAC sub layer frame.

4.1.4. Medium Access Control Layer

The data link layer of the IEEE 802.15.4 standard has two sub-layers: LLC and MAC. The MAC layer is located above the PHY layer. The transmission and reception of a MAC protocol data unit (MPDU) across the PHY layer data service is a vital function of this layer. There are four MAC service interfaces, as shown in Figure 12 [29].

The MAC sub-layer provides two services which are accessed through two service access points (SAPs) [33]:

a) The MAC data service is accessed via MCPS-SAP [33].
b) The MAC management service is accessed via MLME-SAP.

The PHY layer provides two services accessed through two SAPs [33]:

a) Transmission and reception of a PPDU from the PHY medium is accessed via PD-SAP.
b) The PHY management service is accessed via PLME-SAP.

The MAC layer PAN information base (PIB) holds the MAC layer attributes or variables which can be accessed for an application.

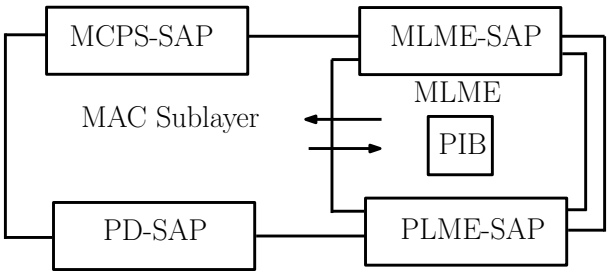

Figure 12. Service interfaces of MAC sublayer.

MAC Superframe Structure

The superframe is employed in the beacon-enabled mode, as shown in Figure 13 [32]. The superframe structure begins with a beacon and is superframe duration *(SD)* symbols long, while the start of two consecutive superframes are beacon interval *(BI)* symbols apart [27]. Each superframe structure is divided into an active period and optional inactive period. The active period is reserved for communication between devices and is followed by the optional inactive period, in which all communications between devices are disabled and devices go to low-power sleep until the arrival of the next beacon frame. The active period is divided into 16 slots, which are further divided into

the contention access period (CAP) and an optional contention free period (CFP). During the CAP, a device that wants to transmit uses the slotted CSMA-CA mechanism. During CFP, devices do not need to compete for the medium access because they use guaranteed time slots (GTS) [34]. The PAN coordinator manages the allocation and de-allocation of GTS.

SD and *BI* are specified using the integers *SO* and *BO*, respectively. *SD* and *BI* are defined by the following formulas [32]:

$$SD = aBaseSuperframeDuration * 2^{(SO)} \tag{4.1}$$

$$BI = aBaseSuperframeDuration * 2^{(BO)} \tag{4.2}$$

In beacon-enabled mode, *BO* and *SO* range from 0 to 14; in non-beacon-enabled mode, *BO* and *SO* are 15.

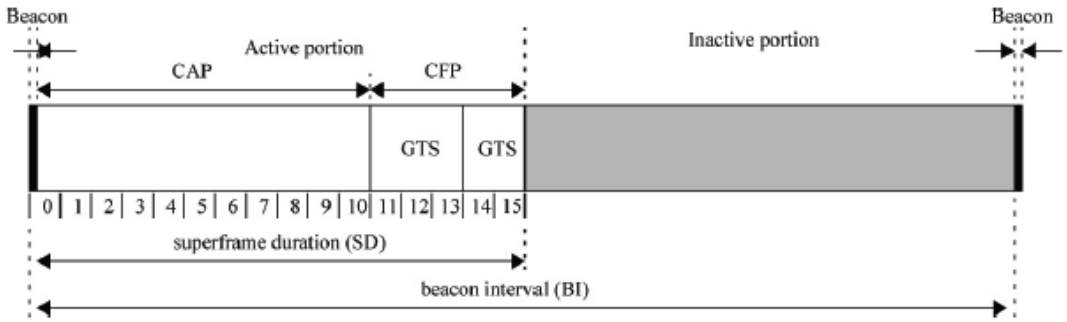

Figure 13. MAC Superframe Structure.

4.1.5. CSMA-CA Mechanism

The MAC layer supports two different modes of operation: slotted CSMA-CA (i.e. beacon-enabled mode) and unslotted CSMA-CA (i.e. non-beacon-enabled mode). Both modes use the CSMA-CA medium access mechanism where devices first check the medium state before starting transmission of the message.

Slotted CSMA-CA Algorithm

In a slotted CSMA-CA, the nodes are synchronised, and the access is slotted. The PAN coordinator transmits beacon packets at periodic *BI* to allow devices to associate with it and synchronise to the superframe structure [35]. Figure 14 [29] shows the slotted version of the CSMA-CA mechanism. The slotted CSMA-CA algorithm is defined by the following steps.

Step 1: Initialise the number of backoffs (NB) = 0, contention window (CW) = 2, and backoff exponent (BE) = 2.

Step 2: After locating a backoff boundary, wait for a random number of backoff periods 0 to $2^{BE} - 1$ before attempting to access the medium [36].

Step 3: After the backoff delay, perform a CCA to verify if the medium is idle or not [36].

Step 4: If the channel is busy, increment *NB* and *BE* values by 1 and start again from step 2.

Step 5: If the channel is idle, decrement *CW* by 1. Transmit the packet when *CW* reaches 0; otherwise, return to step 3.

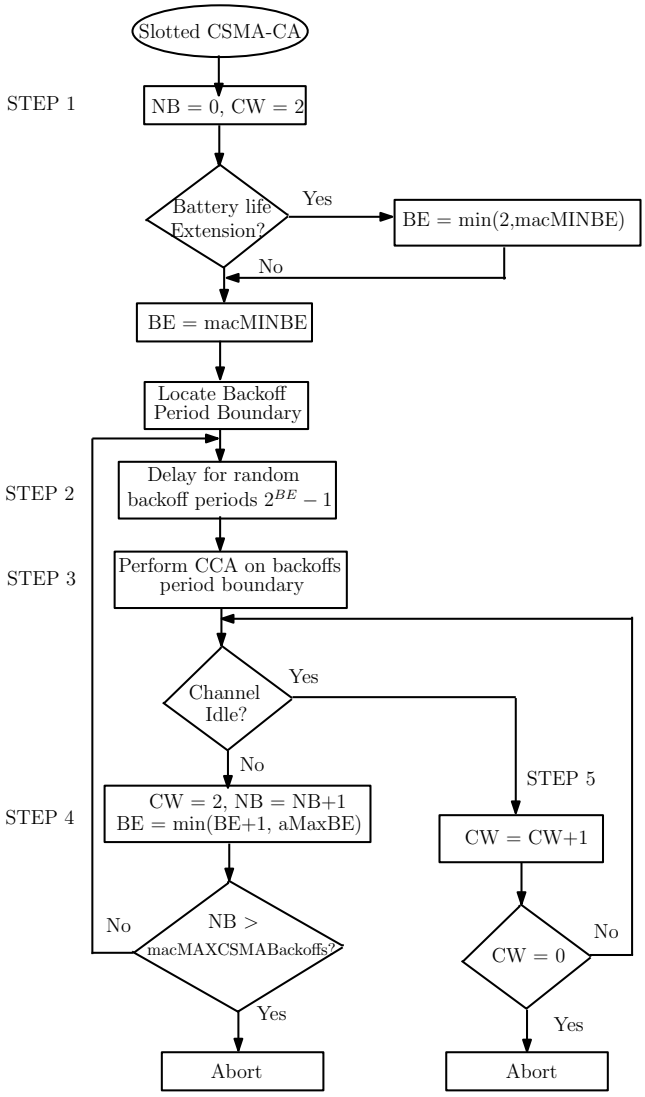

Figure 14. Slotted CSMA-CA algorithm.

Unslotted CSMA-CA Algorithm

The unslotted mode of the CSMA-CA is similar to the slotted CSMA-CA except that the algorithm does not run *CW* number of times when the channel is idle [36, 37]. In

addition, the nodes are not synchronised, and the channel access is unslotted. The PAN coordinator does not transmit beacons unless requested, and the devices communicate with the coordinator using non-beacon-enabled CSMA-CA. The unslotted CSMA-CA algorithm is shown in Figure 15 [29].

Step 1: Initialise variable *NB*.

Step 2: Delay for random backoff period from 0 to $2^{BE} - 1$ [38].

Step 3: Perform CCA.

Step 4: If the channel is idle, transmit the data.

Step 5: If the channel is busy, update variables *NB* and *BE*.

a) If *NB* < *macMaxCSMABackoff*, return to step 2.
b) If *NB* > *macMaxCSMABackoff*, return a failure status.

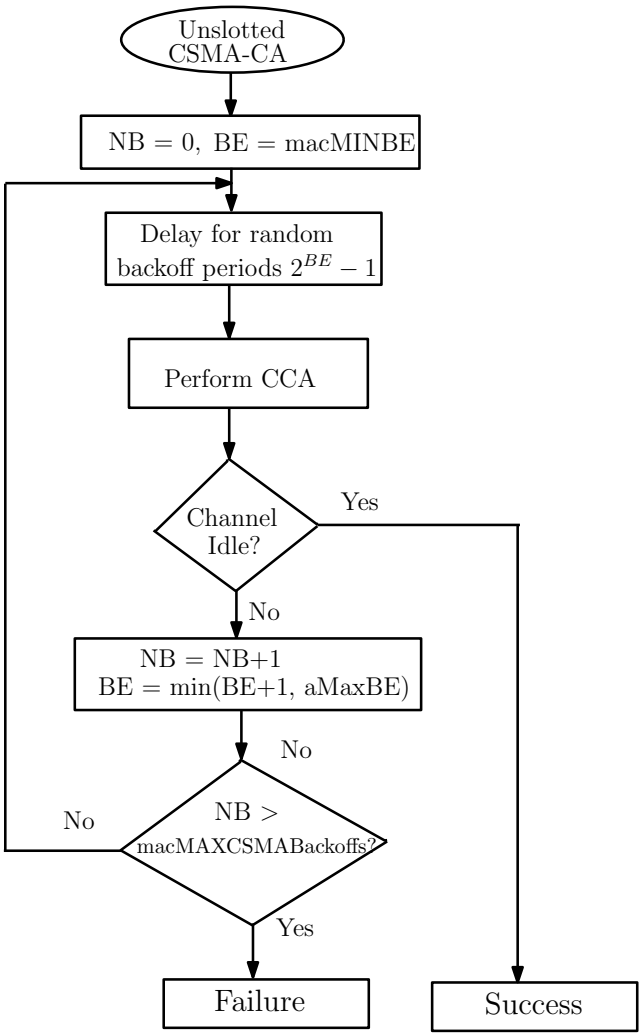

Figure 15. Unslotted CSMA-CA algorithm.

4.2. Markov Analysis: Overview

The Markov chain is a mathematical model in which one state undergoes a transition to another state between a finite number of states [39]. It is a random memoryless process in which the next state is dependent on the current state. Markov analysis views the sequence of events and determines the probability of an event to be followed by another. Using this analysis, random but related sequences are generated which appear similar to the original.

Markov analysis is a powerful analytic tool which can be used to model complex, dynamic, highly distributed, and fault-tolerant systems that would otherwise be very difficult or impossible to model with any other techniques [39, 40]. The Markov technique decreases the task of an analyst by converting the problem from a mathematical computation to state modeling [41]. The Markov model leads to relatively simple models with an insignificant impact on model accuracy.

4.3. Design Mechanism: Markov Chain Analysis of Unslotted IEEE 802.15.4 in Saturation Condition

In the unslotted IEEE 802.15.4 CSMA-CA mechanism, each device has two variables: m and BE. m represents the number of backoffs and is initialised to '0' before every new transmission. BE is the backoff exponent, which indicates the number of backoff periods a device must wait before it can assess the channel [42]. Figure 16 presents the unslotted CSMA-CA Markov chain model of a single device, which can be analysed with the following steps.

Step 1: m and BE are initialised to 0 and BE_{min}, respectively, where BE_{min} is the minimum backoff exponent.

Step 2: The MAC layer waits for a random backoff delay of 0 to $2^{BE} - 1$ [43].

Step 3: The MAC layer requests PHY to perform a CCA.

Step 4: If the channel is assessed to be busy, both m and BE are incremented by 1 to ensure that BE is less than the maximum backoff exponent BE_{max}. If m is less than or equal to the maximum number of retransmissions, the CSMA-CA algorithm must return to Step 2; else, the CSMA-CA terminates the process with a channel access failure status [42].

Step 5: If the channel is idle, the MAC layer starts transmitting the data packets.

The Markov model can be analysed by determining ϕ, which is the stationary probability that the device attempts its CCA. Let $c(t)$ be the stochastic process representing the backoff counter for a random delay at time t [44]. Let $s(t)$ be the stochastic process representing the backoff stages representing the number of times the channel is sensed busy before packet transmission at time t [44]. The two-dimensional Markov chain is

formed with the following transition probabilities:

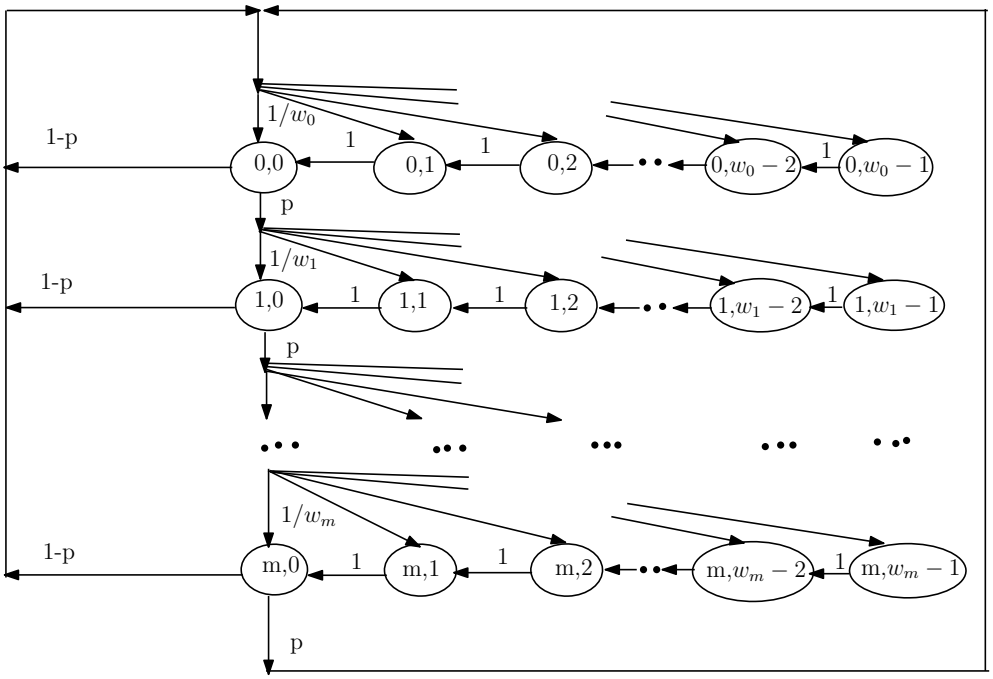

Figure 16. Two-dimensional Markov chain model of unslotted CSMA-CA mechanism for IEEE 802.15.4 in saturation condition.

$$P[i,k|i,k+1]=1, \quad k\in(0,W_i-1), i\in(0,m) \tag{4.3}$$

$$P[0,k|i,0]=\frac{1-p}{W_0}, \quad k\in(0,W_0-1), i\in(0,m-1) \tag{4.4}$$

$$P[i,k|i-1,0]=\frac{p}{W_i}, \quad k\in(0,W_i-1), i\in(1,m) \tag{4.5}$$

$$P[0,k|m,0]=\frac{1}{W_0}, \quad k\in(0,W_0-1) \tag{4.6}$$

Equation 4.3 is the condition to decrement the backoff counter by one unit with probability 1 in every time interval. Equation 4.4 represents the probability that the device senses an idle channel and transmits. The generation of a new frame or retransmission is done with the probability of 1, and one of the initial backoff states is selected with a probability of $\frac{1}{W_0}$. Equation 4.5 shows that, when the CCA detection finds the channel to be occupied, the backoff stage increases, and a new initial backoff value is selected. Equation 4.6 explains that the transmission is terminated when the CCA detection finds the channel to be occupied.

The Markov chain steady-state probabilities can be denoted as follows:
$b_{i,k} = P((s(t), c(t)) = (i, k))$, for $i \epsilon (0, m)$ and $k \epsilon (0, W_i - 1))$.

$$b_{i-1,0} * p = b_{i,0} \quad 0 < i < m \tag{4.7}$$

$$b_{i,0} = p^i * b_{0,0} \quad 0 < i < m \tag{4.8}$$

$$b_{m-1,0} * p = (1 - p) * b_{m,0} = \frac{p^m}{1 - p} * b_{0,0} \tag{4.9}$$

For each $k \epsilon (1, W_i - 1)$,

$$b_{i,k} = \frac{w_i - k}{w_i}, \left| \begin{array}{rl} (1 - p) \sum_{j=0}^{m} b_{j,0} & i = 0 \\ p * b_{i-1,0} & 0 < i < m \\ p * (b_{m-1,0} + b_{m,0}) & i = m \end{array} \right.$$

The sum of the row of the Markov chain matrix is 1 [45]; hence,

$$\sum_{i=0}^{m} \sum_{k=0}^{W_i - 1} b_{i,k} = 1 \tag{4.10}$$

$$\sum_{i=0}^{m} b_{i,0} \sum_{k=0}^{W_i - 1} \frac{W_i - k}{W_i} = 1 \tag{4.11}$$

$$\sum_{i=0}^{m} b_{i,0} \frac{W_i + 1}{2} = 1 \tag{4.12}$$

$$\sum_{i=0}^{m} b_{i,0} W_i + \sum_{i=0}^{m} b_{i,0} = 2 \tag{4.13}$$

where

$$W_i = 2^i * W_{min} = 2^i * W \tag{4.14}$$

By substituting the value of $b_{i,0}$ from equation 4.8, the following equations are obtained:

$$\sum_{i=0}^{m} p^i b_{0,0} 2^i * W + \sum_{i=0}^{m} p^i b_{0,0} = 2 \tag{4.15}$$

$$b_{0,0}[\sum_{i=0}^{m}(2p)^i * W + \sum_{i=0}^{m} p^i] = 2 \tag{4.16}$$

$$b_{0,0}[W\sum_{i=0}^{m}(2p)^i + \sum_{i=0}^{m} p^i] = 2 \tag{4.17}$$

By applying the mathematical series formula [46] given below, the value of $b_{0,0}$ is computed.

$$\sum_{i=0}^{n-1} a^i = \frac{1-a^n}{1-a} \tag{4.18}$$

$$b_{0,0}[W * \frac{1-(2p)^{m+1}}{1-2p} + \frac{1-p^{m+1}}{1-p}] = 2 \tag{4.19}$$

$$b_{0,0}[\frac{W*(1-p)(1-(2p)^{m+1}) + (1-p^{m+1})(1-2p)}{(1-2p)(1-p)}] = 2 \tag{4.20}$$

$$b_{0,0} = \frac{2*(1-p)*(1-2p)}{W*(1-p)*(1-(2p)^{m+1}) + (1-2p)*(1-p^{m+1})} \tag{4.21}$$

To transmit a packet when the given device is performing CCA, all other devices should be in backoff stage. If the channel is idle for the CCA, the transmission state simply follows. ϕ is defined as the conditional probability that the device is in one of the CCA states $(b_{i,0})$. The conditional probability ϕ is defined below:

$$\phi = \frac{\sum_{i=0}^{m} b_{i,0}}{\sum_{i=0}^{m}\sum_{k=0}^{W_i-1} b_{i,k}} \tag{4.22}$$

From equation 4.10, the denominator can be written as $\sum_{i=0}^{m}\sum_{k=0}^{W_i-1} b_{i,k} = 1$. Now, equation 4.22 can be rewritten as follows:

$$\phi = \sum_{i=0}^{m} b_{i,0} \tag{4.23}$$

$$\phi = \sum_{i=0}^{m} p^i b_{0,0} \tag{4.24}$$

$$\phi = b_{0,0} \sum_{i=0}^{m} p^i \tag{4.25}$$

$$\phi = b_{0,0}[\frac{1-p^{m+1}}{1-p}] \tag{4.26}$$

Substitute the value of $b_{0,0}$ from equation 4.21:

$$\phi = \frac{2*(1-p)*(1-2p)}{W*(1-p)*(1-(2p)^{m+1})+(1-2p)*(1-p^{m+1})}[\frac{1-p^{m+1}}{1-p}] \tag{4.27}$$

$$\phi = \frac{2*(1-p^{m+1})*(1-2p)}{W*(1-p)*(1-(2p)^{m+1})+(1-2p)*(1-p^{m+1})} \tag{4.28}$$

Hence, the device is concluded to perform CCA with ϕ. Further, ϕ depends on the state transmission probabilities p and $1-p$, where p is the busy probability of the CCA. It can be calculated using two average numbers: average number t_b of busy slots due to packet transmissions of the other devices and average number t_o of backoff slots a device undergoes to successfully transmit a packet [47].

P_{to} is the probability that a given device does not perform a CCA, which is instead performed by another device; it is defined as follows [47]:

$$P_{to} = (1-\phi)[1-(1-\phi)^{n-1}] \tag{4.29}$$

The successful transmission probability of a node P_{so} is given below [47]:

$$P_{so} = \frac{(n-1)(\phi)[1-(1-\phi)^{n-1}]}{P_{to}} \tag{4.30}$$

The average number of backoff slots t_o can be derived as follows [47]:

$$t_o = \frac{[P_{to}(P_{so}T_{os}+(1-P_{so})T_{oc})+\phi+(1-P_{to}-\phi)]}{\phi(1-\phi)^{n-1}} \tag{4.31}$$

$$t_o = \frac{[P_{to}(P_{so}T_{os}+(1-P_{so})T_{oc})+(1-P_{to})]}{\phi(1-\phi)^{n-1}} \tag{4.32}$$

where $\frac{1}{\phi(1-\phi)^{n-1}}$ is the average number of CCA attempts for a given device to transmit a packet successfully [47], T_{os} is the average number of backoff slots during a

successful transmission, and T_{oc} is the average number of backoff slots during a collision. T_{os} and T_{oc} are calculated as follows:

$$T_{os} = T_s - T_{CCA} \tag{4.33}$$

$$T_{oc} = T_c - \phi \tag{4.34}$$

where T_{CCA} is the time duration to perform a CCA and T_s is the number of occupied slots for successful transmission. These are given as follows [47]:

$$T_s = T_{CCA} + T_L + \delta + T_{ACK} \tag{4.35}$$

where T_L is the time duration to transmit a packet, δ is the time to wait for an acknowledgement, and T_{ACK} is the time to receive an acknowledgement. T_c is the number of occupied slots for a collision and is calculated as follows:

$$T_c = T_{CCA} + T_L \tag{4.36}$$

The average number of busy slots due to packet transmissions of other devices t_b can be calculated as follows:

$$t_b = \frac{P_{to}[P_{so}T_{bs} + (1 - P_{so})T_{bc})]}{\phi(1-\phi)^{n-1}} \tag{4.37}$$

where T_{bs} and T_{bc} are the number of busy slots out of the backoff slots counted for T_{os} and T_{oc}, respectively. T_{bs} and T_{bc} can be defined as follows:

$$T_{bs} = T_{os} - T_{CCA} - \delta \tag{4.38}$$

$$T_{bc} = T_{oc} - T_{CCA} \tag{4.39}$$

The busy channel probability p at a given CCA can be expressed as follows [47]:

$$p = \frac{P_{to}[P_{so}T_{bs} + (1 - P_{so})T_{bc})]}{P_{to}[P_{so}T_{os} + (1 - P_{so})T_{oc})] + 1 - P_{to}} \tag{4.40}$$

4.3.1. Throughput

The saturation throughput of IEEE 802.15.4 is defined as the fraction of time used by the channel to successfully transmit a frame [48]. When n devices are in the backoff states, the probability γ that the device transmits a packet successfully after performing the CCA is $(1-\phi)^{n-1}$ [48]. The saturated throughput can then be derived as

$$S = \frac{n\phi(1-p)\gamma pl}{(1-\phi) + \phi p + \phi(1-p)[\gamma T_s + (1 - \gamma T_c)]} \tag{4.41}$$

where pl is the length of payload in bits.

4.3.2. Delay

The average delay is defined as the sum of the time consumed for backoff operations $E[X]$ and length of the payload pl. The average delay of a node is given as

$$D = E[X]E(slot) + pl \tag{4.42}$$

where $E(slot)$ is the duration of a backoff slot and $E[X]$ is the average backoff delay. The average backoff delay can be calculated as follows:

$$E[X] = \sum_{i=0}^{m} s_i E[W_i] \tag{4.43}$$

where $E(W_i)$ is the average number of successfully transmitted time slots at the $i-th$ backoff stage and s_i is the probability of successfully sending a frame at the $i-th$ stage.

$$E[W_i] = \sum_{k=0}^{i} (W_k + 1)/2 \tag{4.44}$$

$$s_i = \frac{p^i(1-p)}{1-p^{m+1}} \tag{4.45}$$

where $p^i(1-p)$ is the probability of successfully transmitting a frame at the $i-th$ stage. $1-p^{m+1}$ is the probability that the frame is not dropped after the $m-th$ stage [48].

$$D = [\sum_{i=0}^{m} (\sum_{k=0}^{i} \frac{W_k + 1}{2}) \frac{p^i * (1-p)}{1-p^{m+1}} + pl] * E(slot) \tag{4.46}$$

4.3.3. Matlab Simulation Parameters and Results

Table 6 presents the key Matlab simulation parameters of IEEE 802.15.4 such as the number of nodes, payload size, aUnitBackoffPeriod, and channel data rate. CSMA-CA MAC parameters of IEEE 802.15.4 such as the contention window size, maximum backoff, minimum backoff, and retransmissions are also given.

Table 6. MATLAB SIMULATION VALUES

Parameters used in Matlab Simulation	Values
n	25
m	5
BE_{min}	5
BE_{max}	9
pl	1064 bits
$E(slot)$	20 symbols
w	64
T_{CCA}	20 symbols
T_L	72 ms
δ	2 slots
T_{ACK}	32 symbols
1 symbol duration	6 μs
1 slot	0.32 ms
Channel data rate	250 kbps

The Matlab simulation results are presented in visual form in the subsequent figures. The simulation results describe the network throughput and data delay of unslotted IEEE 802.15.4 as a function of the number of nodes.

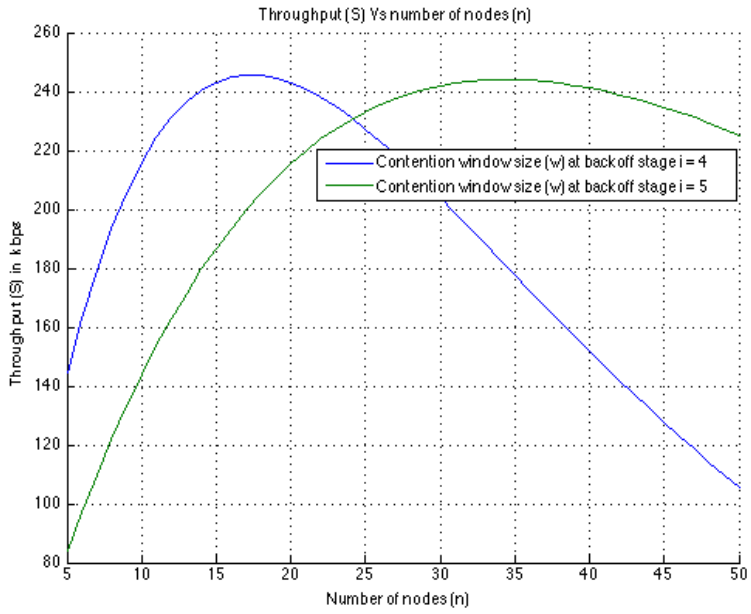

Figure 17. Unslotted IEEE 802.15.4 throughput (S) vs. number of nodes (n = 50) in saturation condition.

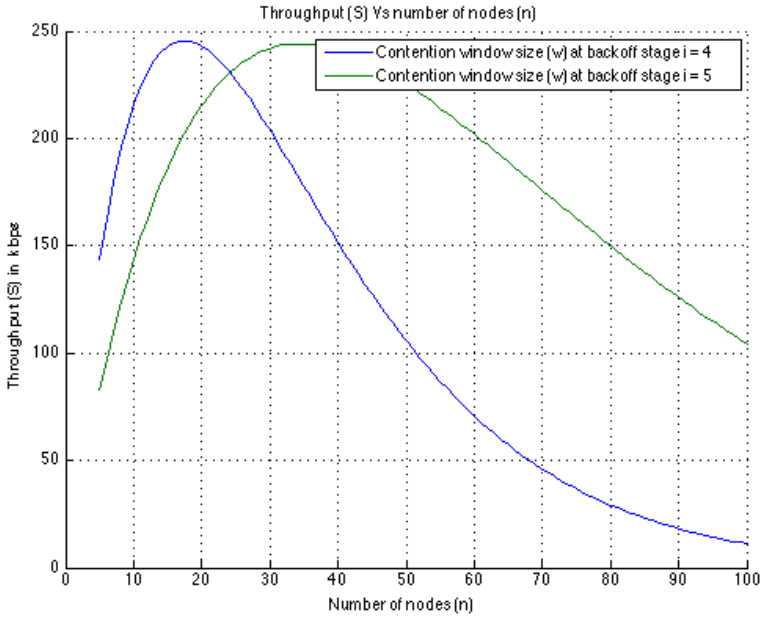

Figure 18. Unslotted IEEE 802.15.4 throughput (S) vs. number of nodes (n = 100) in saturation condition.

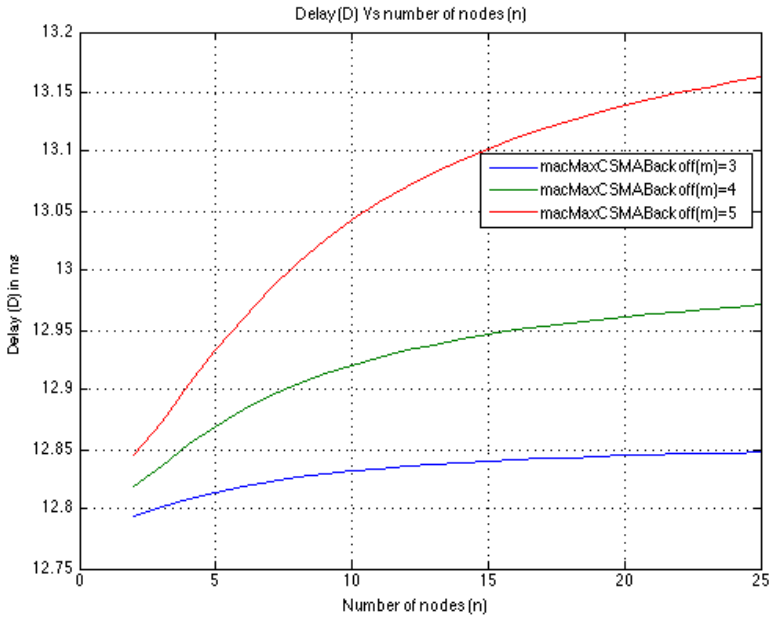

Figure 19. Unslotted IEEE 802.15.4 delay (D) vs. number of nodes (n = 25) in saturation condition.

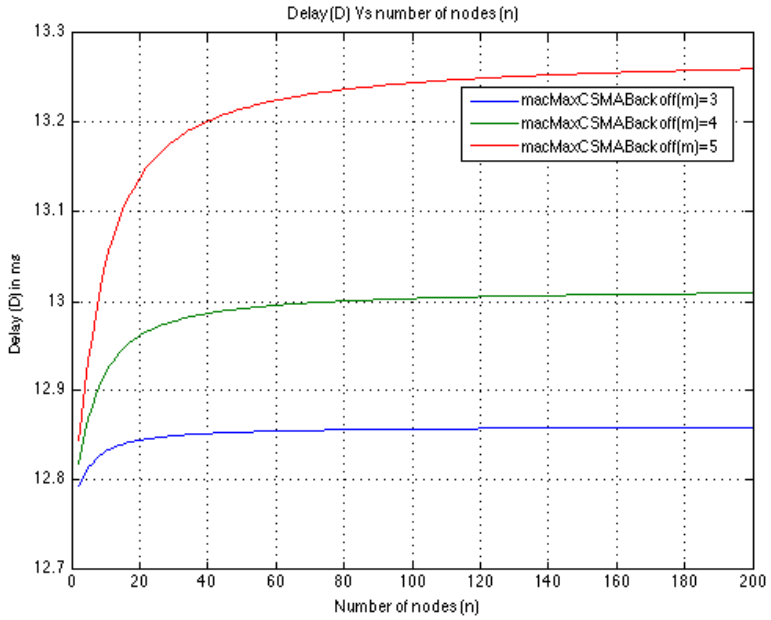

Figure 20. Unslotted IEEE 802.15.4 delay (D) vs. number of nodes (n = 200) in saturation condition.

4.3.4. Discussion

Figure 17 shows the unslotted IEEE 802.15.4 throughput as a function of the number of nodes (n = 50) with a varying contention window size W_i. The throughput initially increases and then starts decreasing as the number of nodes (n = 100) increases, as depicted in Figure 18. As the number of nodes contending for channel access increases, so does the probability of finding a channel busy; therefore, the network throughput starts to decrease. The average throughput with 50 nodes was about 167 kb/s.

The MAC delay is an important factor for smart metering applications. Delay is defined as the total time between the generation of a packet and when the packet is received by the coordinator. Figure 19 presents the data delay of unslotted IEEE 802.15.4 as a function of number of nodes. The delay becomes constant as the number of nodes increases. Figure 20 shows the simulation results; the average delay was over 12 ms.

4.4. Overview of Open-ZB Simulation Model in Opnet

The Open-ZB simulation model version 3.0 in Opnet implements the PHY and MAC layers, which are defined by the IEEE 802.15.4 standard [36]. The simulation model implements the PHY layer at the 2.4 GHz frequency band with 250 kbps data rates [32]. The MAC layer only supports the beacon-enabled mode of the IEEE 802.15.4 standard [36]. The different structural layers of the open-ZB model are briefly described below and shown in Figure 21 [49].

1. The PHY layer consists of the wireless radio transmitter and receiver module in accordance with IEEE 802.15.4 [32]. The PHY layer implements the QPSK modulation scheme with the transmitter power set to 0.1 W.

2. The MAC layer implements slotted CSMA-CA and the GTS mechanism [36]. The MAC layer generates the beacon frames and synchronises the network when a given nodes acts as the PAN coordinator [36, 49].

3. The network layer supports both the cluster-tree and star topologies. The star topology is implemented as a special case of the cluster-tree topology where the network depth is set to 1. The mechanism of the network formation is implemented with default distributed address allocation to all nodes.

4. The application layer consists of the data traffic generator. The traffic sources generate unacknowledged and acknowledged data frames transmitted during the CAP (slotted CSMA-CA) [36, 49].

5. The battery module calculates the consumed and remaining energy [36].

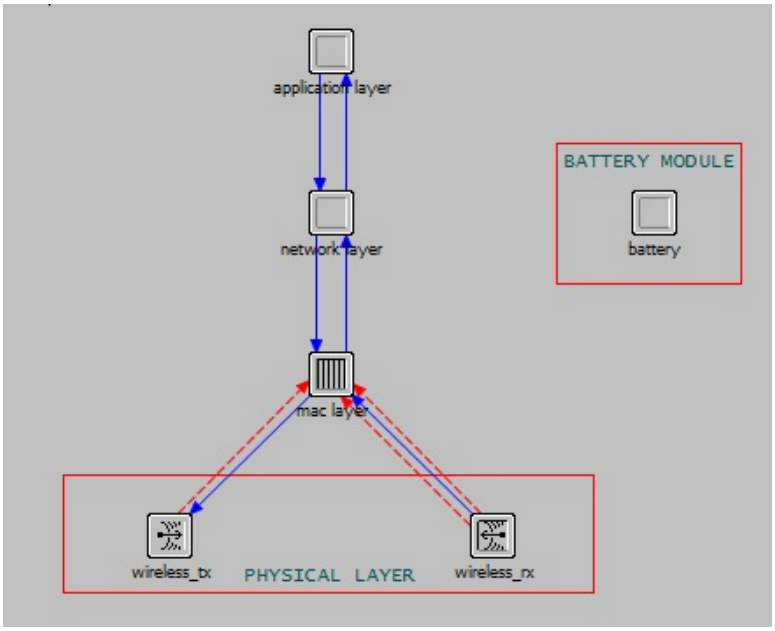

Figure 21. Structure of open-ZB model.

4.4.1. Modification of Open-ZB Model

The Open-ZB simulation model does not implement non-beacon-enabled mode, which is based on the unslotted CSMA-CA mechanism. As a first step, an unslotted CSMA-CA mechanism was added to the previous open-ZB model. Thus, the MAC layer now supports non-beacon-enabled mode. Furthermore, the model can be used to describe a simulation environment which randomises the position of each RTU with respect to

CLH in a cluster. Figure 22 shows the pathloss simulation parameters, which describe the loss in power as radio signal propagates in space. This model was added to the Opnet open-ZB model for other MAC and network parameters.

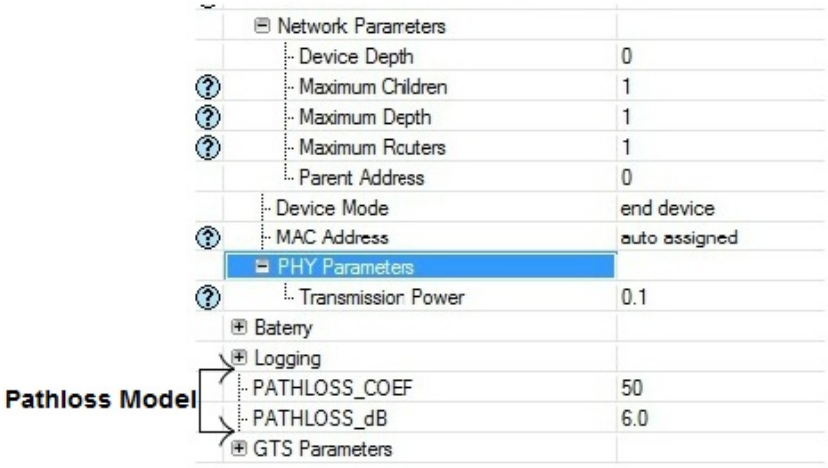

Figure 22. Pathloss simulation parameters.

4.4.2. Opnet IEEE 802.15.4 Simulation Parameters and Results

Table 7 presents key channel coefficients of IEEE 802.15.4 such as the channel bandwidth, transmission power, and data rate. The optimised CSMA-CA MAC parameters of IEEE 802.15.4 such as the maximum backoff, minimum backoff, and retransmissions are also given. The MAC parameters were optimised by trial and error. MAC parameters were selected and compared in the Opnet simulator to find the values best suited for maximum throughput and minimum delay in the SG traffic environment. The MAC parameters were tuned to minimise network delay while maintaining the packet delivery ratio at above 99%, which is a quality-of-service (QoS) requirement for SG AMR traffic [8].

Table 7. OPNET SIMULATION PARAMETERS OF IEEE 802.15.4

Parameters	RTU/CLH
Bandwidth	2 MHz
Base frequency	2400 MHz
Transmitter power	0.1 W
Data Rate	250 kbps
Maximum Backoff Number	9
Minimum Backoff Number	5
Retransmissions	5

The Opnet simulation results are shown in the following figures. The simulation results are for the average end-to-end delay and average network output load, respectively, with normal AMR traffic.

Figure 23. End-to-end delay of unslotted IEEE 802.15.4 in non-saturation condition.

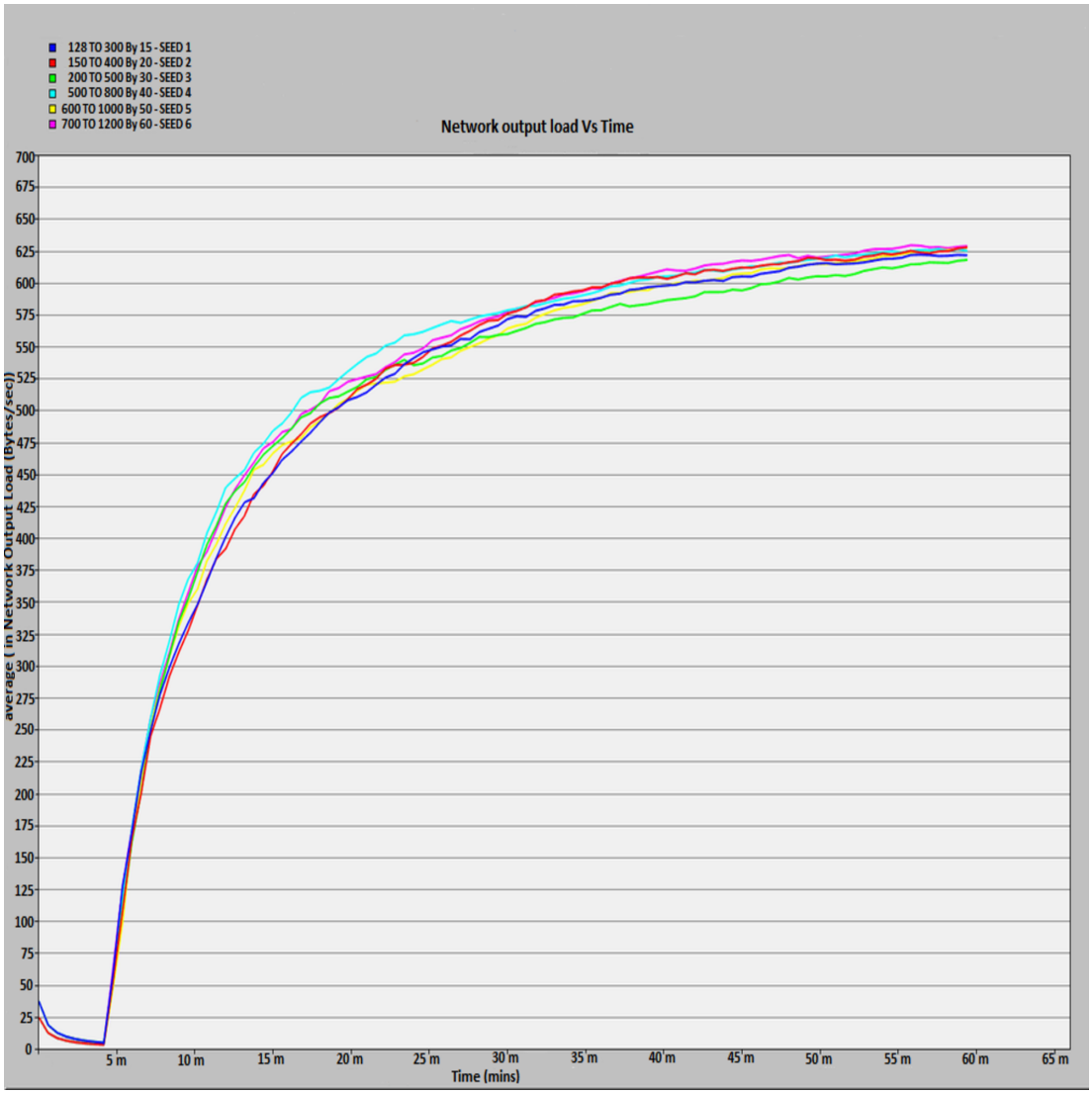

Figure 24. Network output load of unslotted IEEE 802.15.4 in non-saturation condition.

4.5. Discussion

The simulation was run for normal AMR traffic: the data traffic of 25 RTUs with a random start time of 10 min and payload of 250 bytes per RTU. The generation interval of each RTU was 15 min with a simulation duration of 1 h. Figure 23 presents the end-to-end delay (in seconds) as a function of time. The average end-to-end delay increased and then became constant with time. The average end-to-end delay was less than 0.022 s. Figure 24 shows the average network load versus time. The network throughput also increased and became constant with time due to more competition. The average network load was 625 bytes/s.

The results show that the packet delay of IEEE 802.15.4 for the SG communication obtained from Markov chain analysis correlated fairly well with the Opnet modeler simulation results. However, the throughput differed as the Markov chain analysis used saturated traffic conditions and the Opnet simulator used non-saturated traffic

conditions. The simulation results confirmed that the packet delay was below the NIST requirements for smart metering applications.

5. 3GPP LONG TERM EVOLUTION

5.1. Literature Survey on LTE

3GPP LTE is the next evolutionary step in 3G/4G technology [9] to support the continuous demand for high data rates and multimedia services. The LTE network is a bidirectional communications system with wide coverage and improved system capacity. The LTE system is considered to be a leading global standard and platform for an optimised Internet Protocol (IP) radio communication [9].

LTE supports packet-switched mode, and the PHY layer supports multiple scalable bandwidths from 1.4 MHz to 20 MHz in increments of 180 KHz. The maximum data rates are 100 megabits per second (Mbps) for downlink (DL) and 50 Mbps for uplink (UL). LTE supports both frequency division duplex (FDD) and time division duplex (TDD) modes in order to provide enhanced network deployment flexibility [50]. The LTE system introduces new access schemes for the air interface of UL and DL communications: i.e. orthogonal frequency division multiple access (OFDMA) for DL and single carrier-frequency division multiple access (SC-FDMA) for UL [50].

Network Architecture

Figure 25 [51] depicts the LTE network architecture. It is mainly composed of the core network (CN) and radio access network (RAN). The CN consists of an evolved packet core (EPC) and the service domain [52]. The RAN is composed of evolved universal terrestrial radio access (E-UTRAN) and UEs. The EPS provides IP connectivity to the users to connect to a packet data network (PDN). The EPC includes the PDN gateway (P-GW), serving gateway (S-GW), mobility management entity (MME), home subscriber server (HSS), and policy control and charging rules (PCRF) [53].

- P-GW
  The P-GW provides connectivity to the UE to the external networks by acting as a point of entry and exit for traffic [54]. A UE may connect to more than one P-GW.
- S-GW
  The main purpose of S-GW is to route and forward the user data packets. It manages and stores the UE contexts, e.g. an IP bearer service and routing information of a network [53].
- MME
  The MME is a control node for the LTE access network [55]. The key functions of MME involve idle mode UE tracking, bearer activation and deactivation, and choosing the S-GW for the UE.
- HSS
  The HSS includes the user's system architecture evolution (SAE) subscription data and information on the MME. The HSS also contains information about the PDN address [55].

- PCRF
  The PCRF is responsible for the policy control enforcement function of P-GW and authorises the QoS policies.

Service Domain

The service domain offers web browsing and voice and data streaming services to various subsystems in LTE. IP-based multimedia services (IMS) is the main service offered in the service domain. IMS is offered in the LTE network with the Session Initiation Protocol (SIP).

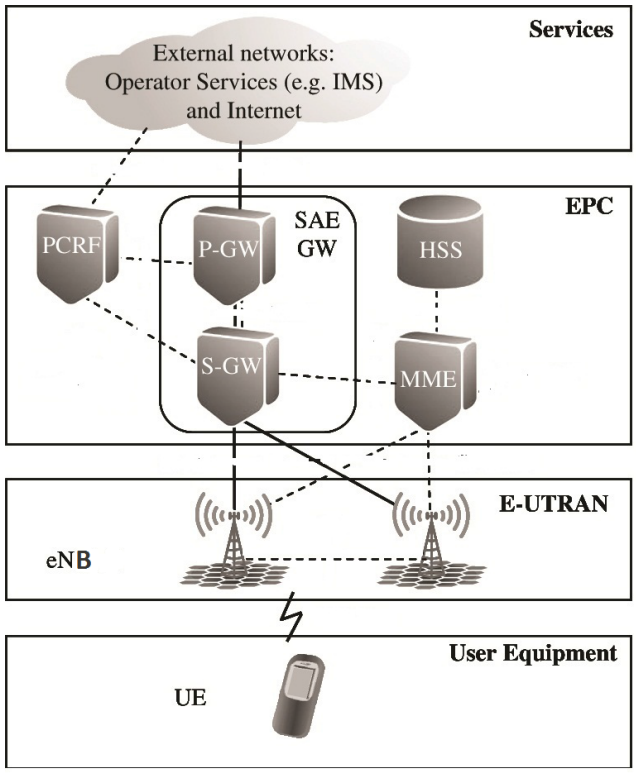

Figure 25. Network architecture of LTE.

5.1.1. E-UTRAN Architecture

Figure 26 [9] presents the architecture of E-UTRAN and EPC. E-UTRAN mainly consists of the evolved node-B (eNB) and access gateway (A-GW). An eNB is a network access element which covers a single cell. eNBs encrypt the user data stream and are connected to each other via the *X2* interface. The MME/SAE gateway connects the eNB and EPC via the *S1* interface. eNB functions include radio admission control, mobility control, and radio bearer control. The core interfaces of LTE are *Uu*, *S1-MME*, *X2*, *S1-u*, and *S5*; these are explained below.

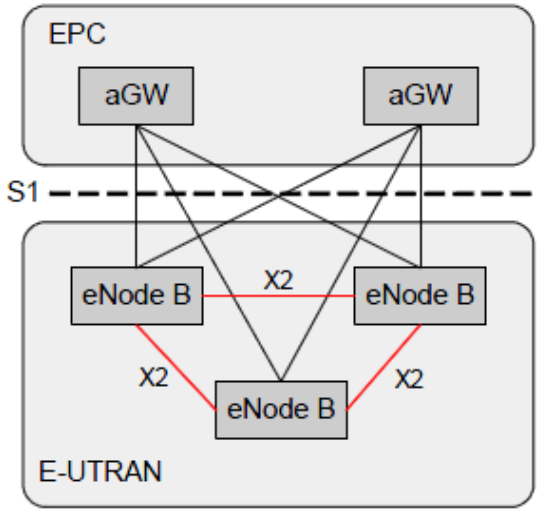

Figure 26. E-UTRAN and EPC architecture.

- LTE *Uu*
  An air interface between the UE and eNB. The Radio Resource Control (RRC) protocol is used for communication between the UE and eNB [9].

- *S1*
  The eNB and MME communicate via this IP interface. The primary task of *S1* is to support network load sharing and traffic redundancy across network elements in the CN [9].

- LTE *X2*
  The eNB communicates with other eNBs via this IP interface.

- LTE *S11*
  An interface between MME and S-GW.

- LTE *S5*
  An IP interface between the S-GW and P-GW with two variants: GPRS tunneling protocol (GTP) interface or proxy mobile IPv6 (PMIP) interface [50].

- LTE *S1-U*
  A user interface between the eNB and SGW [50].

5.1.2. LTE Simulation Parameters

Table 8 [20] presents the key parameters for LTE simulation scenarios [18,20]: channel coefficients such as the antenna gain, bandwidth, and path loss of the RTU and eNB. QoS class identifier number 9 signifies that there is no guaranteed bit-rate (non-GBR) value for the transmitted data [18, 20].

Table 8. KEY SIMULATION PARAMETERS OF LTE

Parameters	RTU	eNB
Tx antenna gain	-2 dBi	16.5 dBi
Bandwidth	10 MHz (UL)	10 MHz (DL)
Transmitter power	0.2 W	39.8 W
Receiver sensitivity	-106.5 dBm	-120.7 dBm
Antenna height	1.5 m	30 m
Base frequency	1800 MHz	1990 MHz
QOS class identifier	9 (non-GBR)	
RLC mode	Acknowledged	
Retransmissions	4	
Scheduling mode	Link adaptation and channel dependent scheduling	
Pathloss	Suburban macrocell, terrain c ,path loss from obstacles -6 dB	

5.2. LTE Traffic Simulation Results

5.2.1. Background Traffic

The average network load and network delay for the chosen background applications in LTE are shown in the subsequent graph plots. Figure 27 [20] shows the average load of the BG traffic applications in LTE as a function of time [18, 20]: a maximum of 750 kB/s from FTP, 300 kB/s from streaming, 30 kB/s from voice, and less than 20 kB/s from HTTP [18, 20].

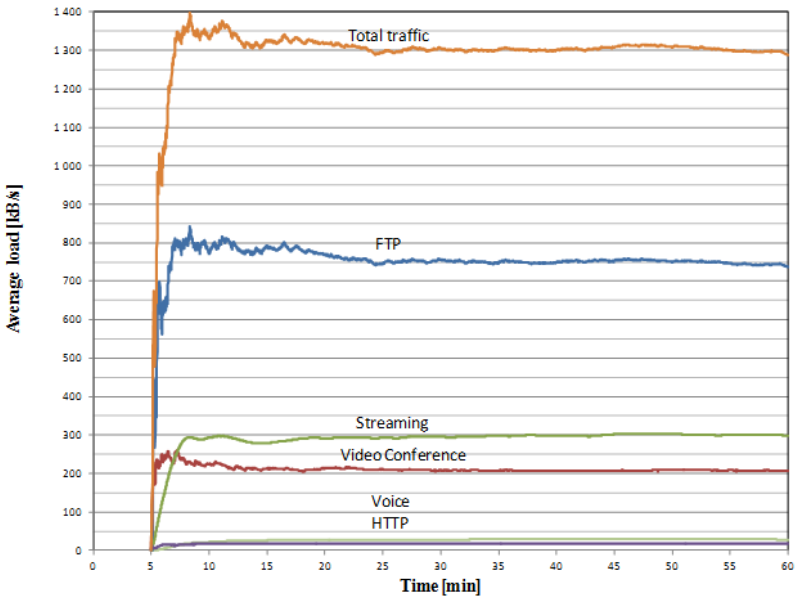

Figure 27. Average load of BG traffic.

Figure 28 [20] signifies the average network delay as a function of time. The network delay was high for FTP application from 10 s to 2 min due to the generated traffic. The voice and video conference delays were clearly less than 100 ms, which is tolerable [20].

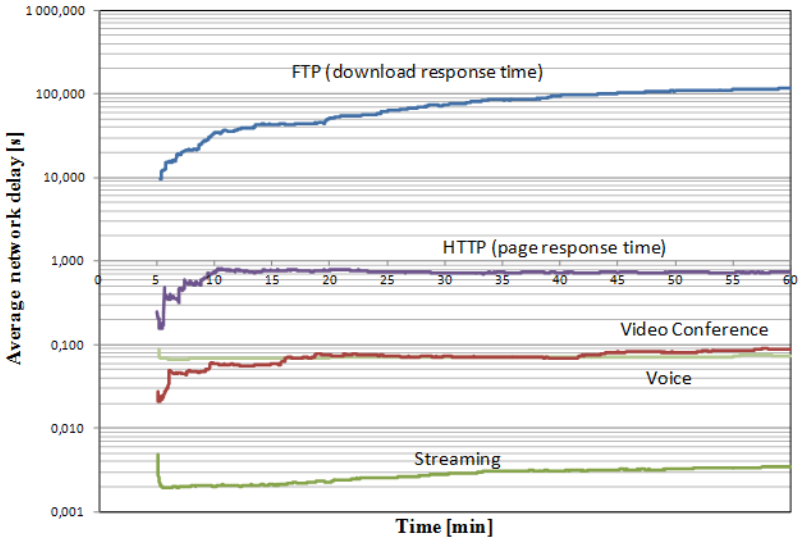

Figure 28. Average network delay of BG traffic.

5.2.2. Normal AMR Traffic with Background Traffic

Figure 29 [20] visualises the average loads of the AMR and BG traffic components. The generated UL and DL traffic of AMR are shown. The generated DL traffic was a bit less than 0.06 kB/s.

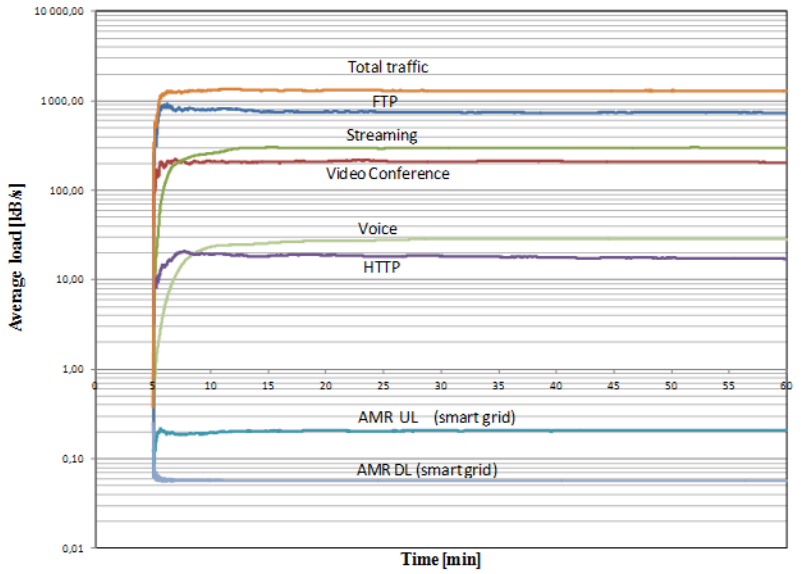

Figure 29. Average load of AMR UL/DL and BG traffic.

Figure 30 [20] depicts the average network delay as a function of time. The DL AMR traffic is compared to the previous BG and normal scenario. The delay for DL AMR was a bit more than 2 ms with low latency.

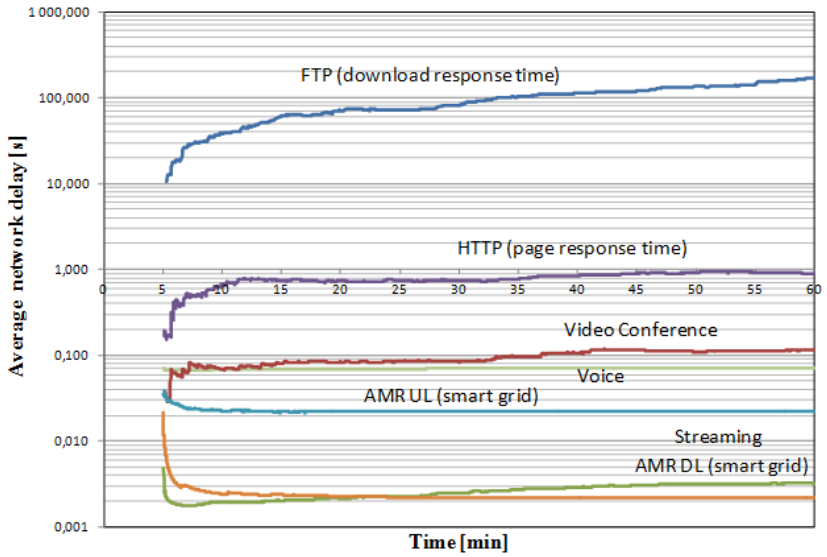

Figure 30. Average delay of AMR UL/DL and BG traffic.

5.3. Discussion

The thesis examined the impact of AMR traffic on regular LTE traffic and vice versa. The simulation results showed that AMR traffic was only a bit more than 0.2 kB/s. Thus, it does not significantly affect the total traffic. The addition of AMR traffic increased the FTP delay by 1 min at most, which is a large increase but not significant [20]. HTTP traffic was delayed by approximately 0.3 ms, which will not impact the user experience. For other regular LTE traffic applications, there was no significant increase in average network delays [15,20]. The simulation results clearly showed that SM traffic does not hinder the LTE network approach; thus, LTE can be a solution for SM communications.

6. CONCLUSION

This thesis presented the optimisation of IEEE 802.15.4 for SG communications and investigated the issues and challenges related to the modelling, analysis, and performance evaluation of LTE and WSN communication networks. This thesis had three parts. First, the effect of SM traffic on the network performances of the LTE and LTE-WSN approaches was analysed. QoS parameters such as the average end-to-end delay and network output load with different MAC parameters were simulated for smart metering application. Second, a dedicated Markov chain model was introduced to describe the network performance of IEEE 802.15.4 for smart metering application. Third, the feasibility of a hybrid LTE-WSN for SM communication was evaluated according to NIST requirements.

The impact of CSMA-CA MAC parameters on the performance of the IEEE 802.15.4 MAC layer was studied under different network environments. IEEE 802.15.4 was originally designed for low data rates and saturated data communication. Thus, CSMA-CA MAC parameters were specified for such network conditions. Since smart metering applications have characteristics which differ from the original purpose of the IEEE 802.15.4 standard, the configuration of IEEE 802.15.4 MAC parameters should be considered to improve suburban SG communication. In order to configure IEEE 802.15.4 MAC parameters, a Markov chain model of IEEE 802.15.4 for smart metering application was introduced and validated through Opnet modeler simulations. Using the Markov chain model for the smart metering application was a novel contribution of this thesis.

The simulation results showed that SM traffic does not significantly affect the network performance of LTE and LTE-WSN. Therefore, pure LTE and hybrid LTE-WSN were concluded to be capable of supporting different types of network traffic, and hybrid LTE-WSN was concluded to be suitable for SG. The simulation results with regard to the data delay and average load values of SM traffic were compared to NIST requirements. As shown in Table 5, the average delay for smart metering requirements should be less than 10 s for payloads ranging from 200 to 1600 bytes with a PDR of 99%. The simulation results validated the feasibility of LTE and WSN communications in accordance with NIST requirements for smart metering applications. Hence, hybrid LTE-WSN can be used for higher network throughput and lower packet delay in smart metering applications.

7. REFERENCES

[1] Cecati C., Mokryani G., Piccolo A. & Siano P. (2010) An overview on the smart grid concept. In: 36th Annual IEEE Conference on Industrial Electronics Society (IECON), pp. 3322–3327.

[2] Feng Z. & Yuexia Z. (2011) Study on smart grid communications system based on new generation wireless technology. In: IEEE International Conference on Electronics, Communications and Control (ICECC), pp. 1673–1678.

[3] Fan Z., Kalogridis G., Efthymiou C., Sooriyabandara M., Serizawa M. & McGeehan J. (2010) The new frontier of communications research: smart grid and smart metering. In: Proceedings of the 1st International Conference on Energy-Efficient Computing and Networking, ACM, pp. 115–118.

[4] Tan S.K., Sooriyabandara M. & Fan Z. (2011) M2M communications in the smart grid: Applications, standards, enabling technologies, and research challenges. International Journal of Digital Multimedia Broadcasting, vol. 2011.

[5] Feng Z., Jianming L., Yuexia Z. et al. (2010) Study on the application of advanced broadband wireless mobile communication technology in smart grid. In: IEEE International Conference on Power System Technology (POWERCON), pp. 1–6.

[6] Gungor V.C., Sahin D., Kocak T., Ergut S., Buccella C., Cecati C. & Hancke G.P. (2011) Smart grid technologies: communication technologies and standards. IEEE Transactions on Industrial Informatics, vol. 7 , pp. 529–539.

[7] Depuru S., Wang L., Devabhaktuni V. & Gudi N. (2011) Smart meters for power grid; challenges, issues, advantages and status. In: Power Systems Conference and Exposition (PSCE), IEEE/PES, pp. 1 –7.

[8] (Last accessed on 01-01-2012) `http://collaborate.nist.govt/wiki-sggrid/bin/view/SmartGrid/PAP02Objective1`.

[9] Dahlman E. (2008) 3G evolution: HSPA and LTE for mobile broadband. Academic Press.

[10] Mao R. & Julka V. (2011) Wireless broadband architecture supporting advanced metering infrastructure. In: 73rd IEEE Vehicular Technology Conference (VTC Spring), pp. 1–13.

[11] Yerra R.V.P., Bharathi A.K., Rajalakshmi P. & Desai U. (2011) WSN based power monitoring in smart grids. In: Seventh IEEE International Conference on Intelligent Sensors, Sensor Networks and Information Processing (ISSNIP), pp. 401–406.

[12] Latré B., Mil P.D., Moerman I., Dhoedt B., Demeester P. & Dierdonck N.V. (2006) Throughput and delay analysis of unslotted IEEE 802.15.4. Journal of Networks 1, pp. 20–28.

[13] Park P., Di Marco P., Fischione C. & Johansson K. (2012) Modeling and optimization of the IEEE 802.15.4 protocol for reliable and timely communications .

[14] Wang B. & Baras J.S. (2011) Performance analysis of time-critical peer-to-peer communications in IEEE 802.15.4 networks. In: IEEE International Conference on Communications (ICC), pp. 1–6.

[15] Markkula J. & Haapola J. (2013) Impact of smart grid traffic peak loads on shared LTE network performance. In: IEEE International Conference on Communications (ICC), pp. 4046–4051.

[16] Xu Y. & Fischione C. (2012) Real-time scheduling in LTE for smart grids. In: 5th IEEE International Symposium on Communications Control and Signal Processing (ISCCSP), pp. 1–6.

[17] Gungor V.C., Lu B. & Hancke G.P. (2010) Opportunities and challenges of wireless sensor networks in smart grid. IEEE Transactions on Industrial Electronics 57, pp. 3557–3564.

[18] Avvaru A. (2013) Evaluation of Long Term Evolution and IEEE 802.15.4k for Suburban Energy Metering. Master's thesis, University of Oulu, Finland.

[19] Hovinen V. & Haapola J. (2011) Propogation models for smart grids communications. Technical Report of Smart Grids and Energy Markets, CLEEN , pp. 1–11.

[20] Haapola J., Markkula J., Avvaru A. & Singh K. (2012) Traffic requirements and dimensioning for smart grids communications. Technical Report of Smart Grids and Energy Markets, CLEEN , pp. 1–20.

[21] Saunders S. & Aragón-Zavala A. (2007) Antennas and propagation for wireless communication systems. Wiley.

[22] Goldsmith A. (2005) Wireless communications. Cambridge University Press.

[23] Rappaport T.S. (1991) The wireless revolution. IEEE Communications Magazine 29, pp. 52–71.

[24] (Last accessed on 15-06-2012) `http://www.opnet.com/solutions/network/modeler`.

[25] Chang X. (1999) Network simulations with OPNET. In: IEEE Simulation Conference Proceedings, vol. 1, pp. 307–314.

[26] Pešović U. (2010) Hidden Node Avoidance Mechanism for IEEE 802.15.4/ZigBee Wireless Sensor Networks. Master's thesis, University of Maribor, Slovenia.

[27] Pešović U., Mohorko J., Benkič K. & Čučej Ž. (2009) Effect of hidden nodes in IEEE 802.15.4/Zigbee wireless sensor networks. In: XVII Telecommunications Forum-TELFOR, pp. 24–26.

[28] Laboratory N.E.T. (2009) Advanced metering infrastructure. NETL Modern Grid Strategy .

[29] (2012) IEEE standard 802.15.4e TM-2012, IEEE Standard for Local and Metropolitan Networks - Part 15.4: Low-Rate Wireless Personal Area Network (LR-WPANS). Amendment 1: MAC sublayer , pp. 1 – 314.

[30] Ech-Chaitami T., Mrabet R. & Berbia H. (2011) Interoperability of LoWPANs based on the IEEE 802.15.4 standard through IPv6. Int J Comput Sci , p. 2.

[31] Rohm D.M. (2009) Dynamic reconfiguration of beaconless IEEE 802.15.4 MAC parameters to achieve lower packet loss rates. Ph.D. thesis, The University of Wisconsin.

[32] (2011) IEEE standard 802.15.4 TM-2011, IEEE Standard for Local and Metropolitan Networks - Part 15.4: Wireless Medium Access Control (MAC) and Physical Layer (PHY) Specifications for Low-Rate Wireless Personal Area Networks (WPANS) , pp. 1 – 314.

[33] Feng L.C., Chen H.Y., Li T.H., Chiou J.J. & Shen C.C. (2010) Design and implementation of an IEEE 802.15.4 protocol stack in embedded linux kernel. In: 24th IEEE International Conference on Advanced Information Networking and Applications Workshops (WAINA), pp. 251–256.

[34] Karapistoli E., Pavlidou F., Gragopoulos I. & Tsetsinas I. (2010) An overview of the IEEE 802.15.4a standard. IEEE Communications Magazine 48, pp. 47–53.

[35] Wang F., Li D. & Zhao Y. (2011) Analysis of CSMA/CA in IEEE 802.15.4. IET Communications 5, pp. 2187–2195.

[36] Cunha A., Koubaa A., Severino R. & Alves M. (2007) Open-ZB: an open-source implementation of the IEEE 802.15.4/Zigbee protocol stack on TinyOS. In: IEEE International Conference on Mobile Adhoc and Sensor Systems (MASS 2007), pp. 1–12.

[37] Latré B., Mil P., Moerman I., Dhoedt B., Demeester P. & Dierdonck N. (2006) Throughput and delay analysis of unslotted IEEE 802.15.4. Journal of Networks 1, pp. 20–28.

[38] Kim E.J., Kim M., Youm S.K., Choi S. & Kang C.H. (2007) Priority-based service differentiation scheme for IEEE 802.15.4 sensor networks. AEU-International Journal of Electronics and Communications 61, pp. 69–81.

[39] Norris J.R. (1998) Markov chains (No. 2008). Cambridge University Press.

[40] Taylor H.M. & Karlin S. (1984) An introduction to stochastic modeling, vol. 3. Academic Press New York.

[41] Wang W., Xu Q., Fang S., Hu H., Rong L. & Du Y. (2009) Performance analysis of unsaturated slotted IEEE 802.15.4 medium access layer. In: IET International Communication Conference on Wireless Mobile and Computing (CCWMC), pp. 53–56.

[42] Ergen S.C., Fischione C., Marandin D. & Sangiovanni-Vincentelli A. (2008) Duty-cycle optimization in unslotted 802.15.4 wireless sensor networks. In: IEEE Global Telecommunications Conference (GLOBECOM 2008), pp. 1–6.

[43] Nuvolone M. (2010) Stability analysis of the delays of the routing protocol over low power and lossy networks. Ph.D. thesis, KTH.

[44] Ergen S.C., Di Marco P. & Fischione C. (2009) MAC protocol engine for sensor networks. In: IEEE Global Telecommunications Conference (GLOBECOM 2009), pp. 1–8.

[45] Faridi A., Palattella M.R., Lozano A., Dohler M., Boggia G., Grieco L.A. & Camarda P. (2010) Comprehensive evaluation of the IEEE 802.15.4 MAC layer performance with retransmissions. IEEE Transactions on Vehicular Technology, vol. 59 , pp. 3917–3932.

[46] Abramowitz M. & Stegun I.A. (1972) Handbook of mathematical functions with formulas, graphs, and mathematical tables. National Bureau of Standards Applied Mathematics Series 55. Tenth Printing .

[47] Park T.R., Kim T.H., Choi J.Y., Choi S. & Kwon W.H. (2005) Throughput and energy consumption analysis of IEEE 802.15.4 slotted CSMA/CA. Electronics Letters 41, pp. 1017–1019.

[48] Lee S.Y., Shin Y.S., Ahn J.S. & Lee K.W. (2009) Performance analysis of a non-overlapping binary exponential backoff algorithm over IEEE 802.15.4. In: Proceedings of the 4th IEEE International Conference on Ubiquitous Information Technologies & Applications (ICUT'09), pp. 1–5.

[49] Jurcik P., Koubâa A., Alves M., Tovar E. & Hanzálek Z. (2007) A simulation model for the IEEE 802.15.4 protocol: delay/throughput evaluation of the GTS mechanism. In: 15th IEEE International Symposium on Modeling, Analysis, and Simulation of Computer and Telecommunication Systems (MASCOTS'07), pp. 109–116.

[50] Myung H. & Goodman D. (2008) Single carrier FDMA: a new air interface for Long Term Evolution, vol. 8. Wiley.

[51] Holma H. & Toskala A. (2011) LTE for UMTS: Evolution to LTE-Advanced. Wiley.

[52] Fulani S. (2011) Physical layer test trials and analysis of call drops and real time throughput versus channel capacity of the Long Term Evolution (4G) technology .

[53] Zyren J. & McCoy W. (2007) Overview of the 3GPP Long Term Evolution physical layer. Freescale Semiconductor, Inc., white paper .

[54] Sesia S., Toufik I. & Baker M. (2009) LTE-The UMTS Long Term Evolution. From Theory to Practice .

[55] Ali N., Taha A. & Hassanein H. (2011) LTE, LTE-Advanced and WiMAX: Towards IMT-Advanced Networks. Wiley.